

AD-A086 837

PARKE MATHEMATICAL LABS INC CARLISLE MASS

F/G 20/14

SPECTRAL ANALYSIS OF SCINTILLATION DATA TAKEN FROM AN AIRCRAFT.--ETC(U)

FEB 80 T B BARRETT

F19628-76-C-0296

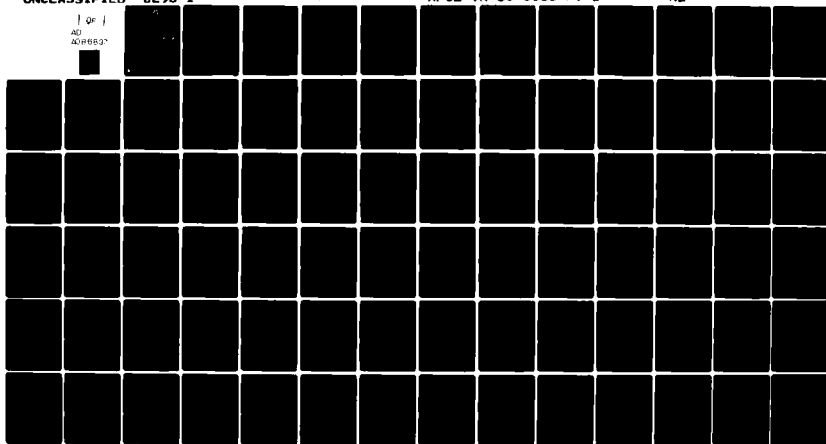
UNCLASSIFIED

0296-1

AFGL-TR-80-0055-PT-1

NL

1 OF 1
AD
A086837



END

DATE

FILED

8-80

DTIC

LEVEL *#*

(12)
SC

AFGL-TR-80-0055(I)

SPECTRAL ANALYSIS OF SCINTILLATION
DATA TAKEN FROM AN AIRCRAFT

Theodore B. Barrett

Parke Mathematical Laboratories, Inc.
One River Road
Carlisle, Massachusetts 01741

Final Report (Part I)
October 1976 - October 1979

February 1980

Approved for public release; distribution unlimited

DTIC
ELECTE
S **D**
JUL 1 8 1980
C

AIR FORCE GEOPHYSICS LABORATORY
AIR FORCE SYSTEMS COMMAND
UNITED STATES AIR FORCE
HANSOM AFB, MASSACHUSETTS 01731

80 7 16 015

ADA 086837

DOC FILE COPY

Qualified requestors may obtain additional copies from the Defense Documentation Center. All others should apply to the National Technical Information Service.

Unclassified

SECURITY CLASSIFICATION OF THIS PAGE (When Data Entered)

19 REPORT DOCUMENTATION PAGE		READ INSTRUCTIONS BEFORE COMPLETING FORM	
1. REPORT NUMBER AFGL-TR-80-00554-PT-1	2. GOVT ACCESSION NO. AD-A086 837	3. RECIPIENT'S CATALOG NUMBER Final Rept. Oct 80 - Oct 83	
4. TITLE (and Subtitle) Spectral analysis of scintillation data taken from an aircraft. Part I.		5. TYPE OF REPORT & PERIOD COVERED Final Report (Part I) 10/76 - 10/79	
7. AUTHOR(s) Theodore B. Barrett		6. PERFORMING ORG. REPORT NUMBER Final Report - 0296-I	
9. PERFORMING ORGANIZATION NAME AND ADDRESS Parke Mathematical Laboratories, Inc. One River Road, Carlisle, MA 01741		8. CONTRACT OR GRANT NUMBER(s) F19628-76-C-0296	
11. CONTROLLING OFFICE NAME AND ADDRESS Air Force Geophysics Laboratory Hanscom AFB, Massachusetts 01731 Contract Monitor: Jurgen Buchau (PHI)		10. PROGRAM ELEMENT, PROJECT, TASK AREA & WORK UNIT NUMBERS 62101F 766309AF	
14. MONITORING AGENCY NAME & ADDRESS (if different from Controlling Office)		12. REPORT DATE February 1980	
		13. NUMBER OF PAGES 81	
		15. SECURITY CLASS. (of this report) Unclassified	
16. DISTRIBUTION STATEMENT (of this Report) Approved for public release; distribution unlimited.		15a. DECLASSIFICATION/DOWNGRADING SCHEDULE	
17. DISTRIBUTION STATEMENT (of the abstract entered in Block 20, if different from Report)			
18. SUPPLEMENTARY NOTES			
19. KEY WORDS (Continue on reverse side if necessary and identify by block number) radio scintillation spectra spectral analysis phase screen model			
20. ABSTRACT (Continue on reverse side if necessary and identify by block number) This report provides theoretical background material for the development of a thin phase screen model for radio scintillation. This model is then used to derive an expression for the expected amplitude scintillation spectra (spectral density function) which might be observed in a geometry which includes a satellite based transmitter, an aircraft based receiver and a thin, intermediate scintillation-producing medium. A computer procedure was developed for testing the model under various geometries and for various parameters describing the "bulk" properties and statistical properties of -			

DD FORM 1 JAN 73 1473

EDITION OF 1 NOV 65 IS OBSOLETE

SECURITY CLASSIFICATION OF THIS PAGE (When Data Entered)

2-16-80

Unclassified

SECURITY CLASSIFICATION OF THIS PAGE(When Data Entered)

the medium.

In addition to the development of a theoretical model, this report includes material on experimental spectral analysis and, in particular, details on a spectral analysis procedure which was used on amplitude scintillation data gathered from an aircraft in geomagnetic equatorial regions.

SECURITY CLASSIFICATION OF THIS PAGE(When Data Entered)

Foreword

This report is the first part of a two-part final report for contract F19628-76-C-0296. Part II, dealing with a 3-D ray trace study, is entitled: "Ground Range and Bearing Error Determination and Display for an OTH Radar Systems with an Arctic Trough Ionosphere".

PM personnel working on the material for this report including software development include:

T.B. Barrett

D. Bandes

S. Newton

The report is incomplete in that time ran out before theoretical results could be properly compared with experimental results. However, we believe the machinery exists, largely in the form of computer software, to perform the calculations necessary to more fully correlate theory and experiment.

Accession For	
NTIS	ORNL
DDC TAB	<input checked="checked" type="checkbox"/>
Unannounced	<input type="checkbox"/>
Justification	<input type="checkbox"/>
By	
Distribution/	
Availability Codes	
Dist	Avail and/or special
A	

TABLE OF CONTENTS

Foreword	iii
Preface	1
Glossary of Symbols Used	3
Introduction	8
Section I - The various domains of scintillation theory	10
Section II - Various approximations for scintillation theory	13
Section III - Second moment properties of the observed field for various approximations	18
Section IV - The thin phase screen approach	23
Section V - A choice of approaches	27
Section VI - Examples	29
Section VII - Overview of spectral analysis	36
References	50
Appendix A - Calculation of Parameter γ, L, ν, α	52
Appendix B - Computation of the theoretical spectra	59
Appendix C - Computation of the spectral density function estimates.	65

Preface

This scientific report can be considered to be mainly on the "spectral analysis of radio wave amplitude scintillations". It attempts to provide both a pseudo-mathematical scenario (model) as the basis of describing and "explaining" certain observations, and what might be best characterized as techniques for relating the model with observations. There are, of course, many physical configurations and parameters which give rise to the phenomenon of scintillation. The basics are a source of electromagnetic radiation (in general, light waves and radio waves can be studied using the same theory). A receiver-detector (usually assumed in the far field of the transmitter) and an intervening medium which is at least partially characterized as having a "random" index of refraction. No one model (herein referred to as general scintillation theory) can, from a practical standpoint, serve to describe all realizations of the above physical configuration nor does it make any sense to try to model the general situation. This report attempts to deal mainly with what has become a "canonical model" (herein referred to as thin screen scintillation theory), i.e., transmitter in free space - "thin" perturbing layer-receiver; both transmitter and receiver many wavelengths from the thin-layer. Details of this model and its range of applicability to reality are discussed in some detail in this report.

No particular attempt is made in this report to justify the study of scintillation in this particular context. It is merely pointed out here that by doing judicious spectral analysis of amplitude scintillation data, it is possible, assuming the validity of the model, to partly characterize the (remote) scintillating layer. From this standpoint, the analysis of radio wave scintillations provide a means of "probing" certain physical characteristics of a remote medium which is difficult and expensive to study by more direct methods (e.g., by going to the medium and measuring electron density). Spectral analysis of scintillation is important by itself, however, since the behavior of scintillation "in the frequency domain" has important consequences for communications systems (though this aspect of scintillation analysis is not discussed further here).

The study of general scintillation theory requires considerable background knowledge in diverse areas of physics and math. For example, electromagnetic wave propagation in general (including optics and radio waves - including waves in a complex ionosphere), stochastic process theory, the theory of propagation in a turbulent medium, communications theory, partial differential equations, and for results, various areas from numerical analysis with emphasis on computer techniques.

Any report reflects first of all the author "modus operandi", i.e., the way he likes to organize and think about things. Secondly, it reflects the author's understanding of the various disciplines which together provide the rational for the topic under study. Finally it reflects the areas of "expertise" where the author has had a reasonable amount of exposure and feels comfortable. This is reflected here by a pre-disposition towards numerical methods and examples.

There is, a vast literature on general scintillation theory and on what is basically thin-screen scintillation theory. Because of this, the subject is rife with a jargon which is meaningful mainly to those who are scintillation specialists which the author is not. Thus, terms like Fresnel filtering, S4 index, etc., etc., are meaningful to scintillation specialists but not to the non-specialists. Thus this report takes some care to define and justify specialized terms which this author, at least, did not find in his hoard of "basic" knowledge. Of course, what is basic to one person is new to another so there is a limit to the "didacity" of any treatise or report. It is not the intent of this report to be a survey article on scintillation but rather to provide for understanding of certain aspects of scintillation under conditions that are made clear in the body of this report.

This report does not include information on an extensive set of computer software which was developed to provide for data reduction (and display). Information on this software is contained in various internal PML reports. Since it is particularly germane to the theme of this Final Report, however, an extensive discussion of the algorithms used for experimental spectral analysis is included.

Glossary of Symbols Used

There is, of course, no standardization of symbols for scintillation theory as described in the abundant literature on the subject. For a single report, however, one must adhere to a consistent symbology. We have chosen to base ours on that which appears in a recent "survey book" on scintillation theory [Ishimaru (1978)]. It differs slightly mainly in the use, or lack of them, of subscripts and/or superscripts.

- ϵ (=dielectric permittivity or just plain permittivity) dielectric constant which describes the propagation medium. In general ϵ is a complex tensor quantity which may depend on field strength. In this report it is always considered to be a real scalar quantity independent of field strength.
- n wave refractive index of the medium (also assumed real) unless specified otherwise.

The relationship $\epsilon = n^2$ is assumed to hold. (see note 1)

- ω wave radial frequency
- λ wave length of electromagnetic field
- k $\frac{2\pi}{\lambda}$ = wave number

(subscript 0 denotes wave number in free space)

$k = k_0 \langle n \rangle$ is assumed where $\langle n \rangle$ = mean wave refractive index.

Note that k is always assumed to be a non-fluctuating quantity - it is a mean wave number in the medium.

- U a (phasor) component of the electromagnetic field (U is generally complex)
- ψ $\ln(U)$ or more exactly $U = \exp(\psi)$. Since U is complex, ψ is.
- χ, S $\psi = \chi + iS$
- z the z -axis is usually used in this report as the predominate line of propagation (typically the transmitter and receiver are placed on the z -axis.) This is in contrast to Ishimaru where he uses the x -axis. (Since many current radio scintillation problems involve looking up to a satellite, the literature on radio scintillation commonly uses the z -axis while light scintillation most commonly uses the x -axis since the propagation of laser beams horizontally through an atmosphere is the typical problem at light frequencies.)

B covariance function ($= \langle \xi(\underline{r}_1) \overline{\xi(\underline{r}_2)} \rangle$) where $\xi(\underline{r})$ is usually a homogeneous random process and \underline{r} is a point in Euclidian space with dimension 2 or greater.

Note that the term correlation function is used by some authors while we choose to reserve the term for $\langle \xi_1 - m, \xi_2 - m \rangle$ where m is the process mean. If the process has zero mean (which it frequently does), there is no distinction between the two terms and they are used interchangeably.

ϕ spectral density function associated with the covariance function B. It is usually assumed that ϕ and B are Fourier transforms of one another.

In this report, the stochastic processes are considered to be "locally" homogeneous. That is to say, at a particular point in space, the correlation function, $B(\underline{r}_1, \underline{r}_2)$, associated with the process depends only on $\underline{r}_1 - \underline{r}_2$. We then write $B(\underline{r}_1, \underline{r}_2) = B(\underline{r}) \equiv B(x, y, z)$ where $\underline{r} \equiv (x, y, z)$ (local coordinates). If, furthermore, the process is isotropic, B is a function of $|\underline{r}_1 - \underline{r}_2|$ which is symbolized by $B(|\underline{r}|)$, $|\underline{r}| = \sqrt{x^2 + y^2 + z^2}$. The following relations hold between the correlation function B and spectral density function ϕ assuming they both exist.

$$\begin{aligned} B(\underline{r}) &= \int_{-\infty}^{\infty} e^{i\underline{K} \cdot \underline{r}} \phi(\underline{K}) d\underline{K} \\ &= \int_{-\infty}^{\infty} \cos \underline{K} \cdot \underline{r} \phi(\underline{K}) d\underline{K} \text{ for real random fields} \\ &\quad \text{since } \phi(\underline{K}) = \phi(-\underline{K}). \end{aligned}$$

$$\phi(\underline{K}) = \frac{1}{(2\pi)^3} \int_{-\infty}^{\infty} e^{-i\underline{K} \cdot \underline{r}} B(\underline{r}) d\underline{r} = \frac{1}{(2\pi)^3} \int_{-\infty}^{\infty} \cos(\underline{K} \cdot \underline{r}) B(\underline{r}) d\underline{r}$$

$$B(|\underline{r}|) \equiv B(r) = \frac{4\pi}{r} \int_0^{\infty} K \phi(K) \sin(Kr) dK$$

$$\phi(|\underline{K}|) = \phi(K) = \frac{1}{2\pi^2 K} \int_0^{\infty} r B(r) \sin(Kr) dr$$

For homogeneous and isotropic stochastic fields, there is an associated (1-dimensional) stochastic process. The relationship between $\phi(K)$ and the spectral density function, $F(K)$, associate with this process is:

$$\Phi(K) = -\frac{1}{2\pi K} \frac{dF(K)}{dK}$$

$$F(K) = 2\pi \int_0^\infty K \Phi(K) dK$$

For the specific case of "frozen-in" turbulence, the following relationship exists between $\Phi(K)$ of the assumed homogeneous and isotropic stochastic field moving with mean speed v , and the spectral density function of the "observed" stationary stochastic process:

$$S(\omega) = \frac{2\pi}{v} \int_{|\omega|/v}^\infty \Phi(K) K dK$$

$$\Phi(K) = \frac{-v^2}{2\pi K} S^1(Kv)$$

where

$$S^1(\omega) = \frac{dS(\omega)}{d\omega}$$

The following useful relationships exist between $B(\underline{r})$, $\Phi(K)$ and $B(x, \underline{\rho})$, $F(x, \underline{\kappa})$:

$$B(x, \underline{\rho}) = \int_{-\infty}^\infty F(x, \underline{\kappa}) e^{i\underline{\kappa} \cdot \underline{\rho}} d\underline{\kappa}$$

$$F(x, \underline{\kappa}) = \frac{1}{(2\pi)^2} \int B(x, \underline{\rho}) e^{-i\underline{\kappa} \cdot \underline{\rho}} d\underline{\rho}$$

$$F(x, \underline{\kappa}) = \int_{-\infty}^\infty \exp(iK_x x) \Phi(\underline{K}) dK_x$$

$$\Phi(\underline{K}) = \frac{1}{2\pi} \int_{-\infty}^\infty \exp(-iK_x x) F(x, \underline{\kappa}) dx$$

If $B(x, \underline{\rho}) = B(x, |\underline{\rho}|)$, then cylindrical coordinates can be used to obtain

$$B(x, |\underline{\rho}|) \equiv B(x, \rho) = 2\pi \int_0^\infty J_0(K\rho) F(x, \kappa) \kappa d\kappa$$

$$F(x, |\underline{\kappa}|) \equiv F(x, \kappa) = \frac{1}{2\pi} \int_0^\infty J_0(K\rho) B(x, \rho) \rho d\rho$$

r a generic point in Euclidian "geometric" space of dimension 3.
K a generic point in Euclidian "transform" space of dimension 3.
ρ a generic point in Euclidian "geometric" space of dimension 2.
κ a generic point in Euclidian "transform" space of dimension 2.
r_e classical radius of the electron $\equiv \frac{e^2}{mc^2} = 2.82 \times 10^{-13} \text{cm}$ (see Jackson (1962), p. 490). This constant appears frequently in the literature because of the relationship between the index of refraction n and the electron density N in a plasma medium where magnetic field and collisions can be neglected. This relationship is:

$$n = (1-X)^{1/2} \text{ where } X = \frac{\omega_p^2}{\omega^2} \text{ where } \omega_p \text{ is the plasma frequency} \equiv \frac{4\pi Ne^2}{m}$$

(Gaussian units) and ω is the radial frequency of the electromagnetic wave. For small X (n close to unity) we obtain

$$n-1 \approx -\frac{X}{2} = -\frac{2\pi Ne^2}{m} \left(\frac{\lambda}{2\pi c}\right)^2 = -\frac{\lambda^2 N}{2\pi} \left(\frac{e^2}{mc^2}\right) = -\frac{\lambda^2 N}{2\pi} r_e$$

note 1 - For a stochastic propagation media, the fluctuations in the quantities which describe the media are usually assumed to be small. If x is the symbol for the stochastic quantity, it is customary to write

$$x = \langle x \rangle (1 + \delta x) \text{ or } x = \langle x \rangle (1 + x_1)$$

where x or x_1 is very small relative to 1 and $\langle \delta x \rangle = \langle x_1 \rangle = 0$. The relationship between $\delta \epsilon \approx \delta n$ follows from

$$\epsilon = \langle \epsilon \rangle (1 + \delta \epsilon)$$

$$n = \langle n \rangle (1 + \delta n) = \sqrt{\frac{\epsilon}{\epsilon_0}} = \sqrt{\frac{\langle \epsilon \rangle (1 + \delta \epsilon)}{\epsilon_0}}$$

If $\langle \epsilon \rangle \approx \epsilon_0$, the free space permittivity, and $\langle n \rangle \approx 1$, we find $1 + \delta n = \sqrt{1 + \frac{\delta \epsilon}{\epsilon_0}}$ or $\delta \approx \frac{\delta \epsilon}{2\epsilon_0}$ or $\delta \approx 2\delta n$. Thus it is permissible to equate, for example, second moment properties of the fluctuating component of permittivity with that of the refractive index, except for a factor of 2.

E electric field. Specifically $\underline{E} = \underline{E}(\underline{r})$ (\underline{E} is a complex vector quantity).

$\left. \begin{matrix} X \\ Y \\ A \\ \phi \\ s \end{matrix} \right\}$ The received (narrow band) signal is $s(t)$ basically $R[U(t)e^{i\omega t}]$ where $U(\underline{r})$ becomes $U(t)$ due to relative motion of transmitter, receiver and the gross medium. The following relations hold:

$$U(t) = X(t) + iY(t) = A(t)e^{i\phi(t)}$$

$$s(t) = X(t)\cos\omega t - Y(t)\sin\omega t$$

$$A(t) = [X^2(t) + Y^2(t)]^{1/2}$$

$$\phi(t) = \tan^{-1} Y(t)/X(t)$$

a quadratic detector produces $A^2(t) = |U(t)|^2$;

a linear detector produces $A(t) = |U(t)|$;

a coherent (linear) detector produces $X(t)$ and $Y(t)$ from which $A(t)$ and/or $\phi(t)$ can be determined.

Introduction

In this report, a basis for explaining certain results from radio wave amplitude scintillation measurements are reported on. The measurements were made from an aircraft flying mainly in (magnetic) equatorial areas with the transmitter located in a satellite. Some of the results of these experiments have been reported on elsewhere (see for example AFGL (1978)). These reports emphasize some of the gross features of the observed scintillation and their relationship to other scintillation measurements from ground observations, and their relationship to other observations of the perturbing medium. The emphasis in this report is on spectral analyses of the measurements. It attempts to provide a model in which to imbed these analyses as well as to displaying some of the results of the analyses.

The report starts out by showing a result by deWolf (1975) from general scintillation theory which attempts to graphically delimit the currently accepted models which appear to be useful in the study of scintillation. This is followed by a brief description of the various theories with emphasis on the thin-screen theory since this latter theory is the one chosen to be used here.

The "canonical" thin-screen scintillation theory is then described for the general configuration and relationships between the spectra which characterize the perturbing medium and those of the observed amplitude scintillations are presented. (These results are mainly those developed by others, e.g., Taylor (1975).) In general, the equations which result are not amenable to solution by "analytical" means, i.e., they remain as complicated integral expressions which are not particularly open to intuitive interpretation. However, some results of numerical integration are presented.

The canonical model is then "computerized", so to speak, for the specific physical configurations realized by the satellite-thin screen-aircraft combination. Here the emphasis is on providing for the transition between the predominantly spatially varying propagation medium (electron density fluctuations) and the temporarily varying radio wave amplitude observations (amplitude scintillations).

This is followed by a brief synopsis of the art of spectral analysis with emphasis on the method used for results presented herein.

In summary, this report provides a source (or reference to a source) of the background material required to bridge the gap between the theory of scintillation spectra and such spectra observed experimentally. In particular, the report leads, on the one hand, to the development and demonstration of a computer procedure for producing model spectra and, on the other hand, to the development of data reduction techniques for producing the experimental spectra to be compared with the model ones.

What remains to be done, and which hopefully will be documented in a subsequent report, is to attempt, first of all, to find good fits between model and experiment and, secondly, to determine the sensitivity of the experimental technique to changes in various model parameters. Thus, typically, one might investigate how (or if) "tomograph techniques" (scan the scintillation in different directions) can resolve various layer parameters such as speed, direction of motion, anisotropy, etc. Going further, how do the multitude of parameters tend to obfuscate the results? Is it really possible to state that the observed spectrum comes from a "power law layer" as opposed to a "Gaussian or Kolmogorof layer"?

Section I - The various domains of scintillation theory

[From D.A. deWolf (1975)]

Before summarizing some of the theoretical methods which are used to study general scintillation theory, it is worthwhile to present a figure which attempts to show the domains of applicability of various theories (which might be better termed approximation techniques). In addition, this figure shows approximately the difference between the "domains of interest" of most optical and radio wave problems. Perhaps the most important feature of this figure is that the domains are 2-dimensional, i.e., defined by two scale parameters. One parameter (the vertical axis) represents the "number of mean free paths" of scattering and thus delimits "single scatter" regions from "multiple scatter" regions. It is, of course, dependant on the statistical properties of the scattering medium. The other parameter (a length) is merely the Fresnel distance associated with the problem. The model on which this diagram is based is very simple, i.e., a plane wave perpendicularly incident on a "slab of turbulence" and a receiver at distance L within the slab. The turbulent slab is characterized by isotropic and homogeneous turbulence such that the spectrum associated with refractive index variations about the mean level is the Kolmogorov spectrum given by

$$\begin{aligned} \Phi_n(\underline{k}) &= .033 C_n^2 |\underline{k}|^{-11/3} & 2\pi L_0^{-1} < |\underline{k}| < 2\pi l_0^{-1} \\ &= 0 & |\underline{k}| > 2\pi l_0^{-1} \end{aligned}$$

and is "undefined" for $0 < |\underline{k}| < 2\pi L_0^{-1}$. C_n is the structure constant which is related to the variance of the refractive index variations by (see Ishimaru (1978) p. 543)

$$C_n^2 = 1.91 \langle \delta n^2 \rangle L_0^{-2/3}$$

The mean free path associated with this spectrum is

$$\alpha^{-1} = [(.033)(1.91) \langle \delta n^2 \rangle L_0^{-2/3} k^2 \int_0^\infty K K^{-11/3} dK]^{-1}$$

where $K \equiv |K|$

Since $\Phi_n(K)$ is not defined between 0 and $2\pi L_0^{-1}$, we use the expedient of integrating between $2\pi L_0^{-1}$ and ∞ with the result

$$\int_{2\pi L_0^{-1}}^\infty K^{-8/3} dK = \frac{3}{5} (2\pi)^{-5/3} L_0^{5/3}$$

$$\text{Thus } \alpha^{-1} \approx 566 \langle \delta n^2 \rangle^{-1} k^{-2} L_0^{-1}$$

The now classic Kolmogorov spectrum for refractive index fluctuations caused by turbulence is characterized by an outer scale length L_0 and an inner scale length l_0 , the idea being that energy is transferred within the "inertial sub-range" from large turbulent blobs of scale size L_0 down to very small blobs of size l_0 beyond which energy is dissipated by molecular collisions. Such a model seems to be well confirmed for a non-plasma atmosphere but probably is not valid for a plasma and in particular, for the ionosphere. None the less, the essential structure of the diagram should remain valid.

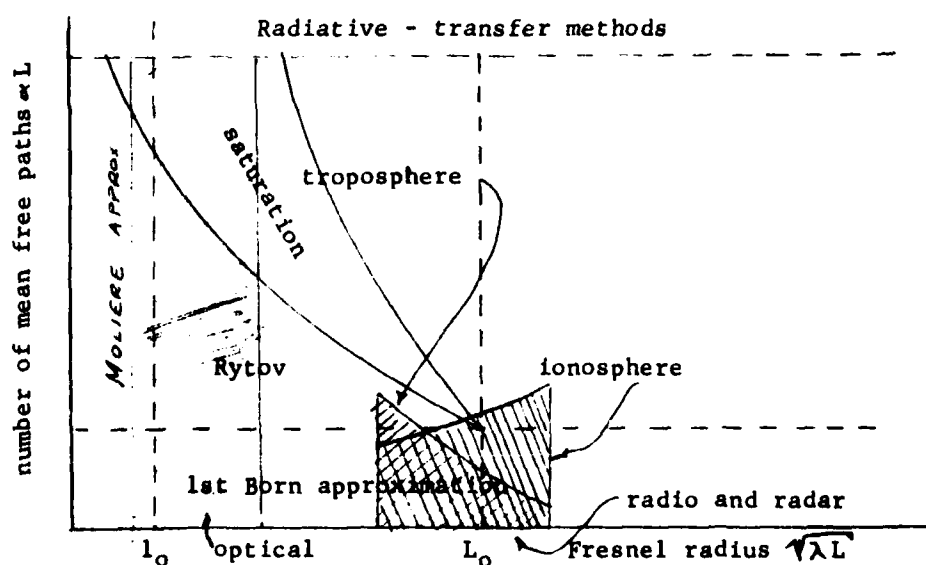


Figure 1. Scintillation approximation regimes (No scale but imagine logarithmic scales.)

Note that many of the approximations used in scintillation actually were developed for scattering problems in quantum mechanics since the Schroedinger equation can be made identical to the scalar wave equation. The Moliere approximation is valid for small angle scattering (see, for example, Modesitt (1971) and associated references).

It should be emphasized that this diagram applies only to the simple model as stated and the thin phase screen which we choose to emphasize later is not really in this diagram (perhaps other dimensions should be added to take account of more geometries). None the less, it serves as an introduction to some of the approximations which are briefly discussed next.

Section II - Various approximations for scintillation theory

General (wave) scintillation theory is imbedded in a more inclusive theory called wave scattering in a stochastic medium. This theory has at least two main branches (transport theory might be considered to be a third): discrete scattering theory, where the scatterers usually have well defined boundaries and are imbedded in a homogeneous medium; continuum scattering where the parameters of the medium vary continuously but stochastically in space and/or time. An overview of much of wave scattering theory is presented in Ishimaru (1978).

The continuum theory is appropriate in the study of line of sight radio wave propagation through a layer of refractive fluctuations. This theory in turn has developed along several paths. Two which predominate the study of radio wave propagation phenomena are the "scattering cross section approach" and the "scalar wave equation" approach. In the first method, a stochastic scattering cross section is defined over a volume of propagation space and the statistical characteristics of the observed field (usually far from the scattering volume) are obtained directly from formulations of the scattering cross section. This method is a generalization of a similar procedure used for discrete scatterers. (See, for example, Ishimaru (1978), Chapter 2 and Chapter 16.)

In the second method, which is generally used for line of sight propagation, the starting point is a stochastic differential equation. The differential operator may operate on either a vector or scalar field but because of obvious computational considerations, most useful results which have been obtained are for scalar fields. In recent years, a vast literature has appeared on various approximate solutions to the stochastic scalar wave equation. This literature has its practical origins in the area of laser communications systems on the one hand and satellite radio wave communication systems on the other hand. This theory is generally referred to as "wave propagation in a turbulent medium" wherein it is usually implied that propagation is essentially in the forward direction as opposed to "scatter propagation" wherein the communication path is distinctly bent. (Gross refractive effects may occur in "wave propagation" however.) As the name implies, the fluctuations or "irregularities" in the propagation medium are due primarily to turbulence. Thus,

turbulence theory must be invoked to explain the statistical characteristics of the fluctuations (of the refractive index, for example).

The remainder of this section is devoted mainly to summarizing pertinent results (or approximations) from this theory - referred to below simply as stochastic wave theory. Before doing so, however, it is pertinent to point out that stochastic wave theory (as mentioned previously) is a subset of the mathematical theory of stochastic differential and integral equations, or more simply, statistical continuum theories. In Beran (1968), some useful generalities concerning this theory are presented with examples of solution methods in different physical regimes. Beran points out some of the general difficulties in solving these equations. Because of these difficulties, the equations for the stochastic fields themselves are not solved but rather equations for various statistical moments are solved for (typically using various approximation methods). The method most commonly used in stochastic wave theory is to obtain an integral equation "solution" for the wave equation and to then determine the various moments.

The starting point for stochastic wave theory is the stochastic differential equation for electric field \underline{E} : (in general, \underline{E} is a complex vector quantity)

$$\nabla^2 \underline{E} + k_0^2 n^2 \underline{E} - 2 \nabla \left(\frac{\nabla n}{n} \cdot \underline{E} \right) = 0 \quad (2-1)$$

See, for example, Tatarski (1961) or Ishimaru (1978). Particular note should be made of the fact that the refractive index, n , is a scalar function of position (and possibly time) only, so that the medium is assumed to be isotropic in the non-statistical sense of the term. (The fluctuations of refractive index may be anisotropic in the statistical use of the word, i.e., the function $B(\underline{r}_1, \underline{r}_2) = \langle n(\underline{r}_1) n(\underline{r}_2) \rangle$ may be a function of $r \equiv |\underline{r}_1 - \underline{r}_2|$ only.) Under certain conditions (usually assumed), the last term in equation (2-1) can be neglected. Physically this means that polarization effects can be neglected since there is no coupling between the vector character of the electric field and the vector electron density gradient. The simplifying assumption is that $\lambda \ll l_0$ where l_0 is the "scale size" of the stochastic medium. Typically, this scale size is defined by $B_n(r) = C \exp(-r/l_0)$ assuming that the correlation function for n , B_n , has the above form. Other forms for B_n can usually be used to define a similar scale size. With this approximation (2-1) can be simplified to the (scalar) Helmholtz equation (see e.g., Born and deWolf (1964) or Jackson (1962)).

$$(\nabla^2 + k_0^2 n^2)U = 0 \quad (2-2)$$

where U is a component of the electric field vector transverse to the mean propagation path. A "solution" to this equation (actually the integral equation form) is found using the outward radiating free space Green's function (e.g., see Frisch (1968)).

$$U = G^0(\underline{r}, 0) - k_0^2 \int_V G^0(\underline{r}, \underline{r}^1) \mu(\underline{r}^1) U(\underline{r}^1) dV^1 \quad (2-3)$$

where

$$k^2 \mu = k_0^2 (n^2 - \langle n \rangle^2) \quad (2-3a)$$

$$G_0(\underline{r}, \underline{r}') = \frac{\exp(ik_0 |\underline{r} - \underline{r}'|)}{-4\pi |\underline{r} - \underline{r}'|} \quad (2-3b)$$

In order to truly solve such an expression for U it is necessary to put bounds on the region of integration V and to approximate U (the unknown) within the integral. Various formal solution methods to 2-3 are given in the above reference. For many applications the Born approximation, sometimes referred to as the "single-scattering" approximation, is made whereby the unknown field component, U , is replaced by the free space field U_0 . Another technique is to assume the form $U(\underline{r}) = W(\underline{r})e^{ikz}$ for a wave propagating in the positive z direction and where $W(\underline{r})$ is a function which varies, at most, slowly in the z -direction. Then the Helmholtz equation is written as:

$$2ik \frac{dW}{dz} + \nabla^2 W + k^2 \delta n^2 W = 0 \quad (2-5)$$

where

$$k_0^2 n^2 = k^2 (1 + \delta n^2)$$

Then, assuming the above mentioned scaling condition, $\lambda \ll l_0$, it can be shown that

$$|k \frac{dW}{dz}| \gg \left| \frac{d^2 W}{dz^2} \right|$$

and the following approximate parabolic equation for W is obtained:

$$2ik \frac{dW}{dz} + \left(\frac{d^2}{dx^2} + \frac{d^2}{dy^2} \right) W + k^2 \delta n^2 W = 0 \quad (2-6)$$

Another approximation, the Rytov approximation, is obtained by first making the substitution $U(\underline{r}) = \exp(\psi(\underline{r}))$ and writing $\psi = \psi_0 + \psi_i$ where ψ_0 is the free space component of ψ and ψ_i is that due to the irregularities. The equation for ψ_i is:

$$(\nabla^2 + k^2)U_0 \psi_i = [\nabla\psi_i \cdot \nabla\psi_i + k^2 dn]U_0$$

where $U_0 = e^{\psi_0(\underline{r})}$ or $\exp(\psi_0(\underline{r}))$ is the free space "component" of the field and $dn = (1 + \delta n)^2 - 1$. The Rytov approximation ignores terms in $\nabla\psi_i$ with the result that the following integral equation for ψ_i can be derived (see, for example, Ishimaru (1978) or Yeh and Liu (1972)):

$$\psi_i(\underline{r}) = \frac{k^2}{U_0(\underline{r})} \int_V G^0(\underline{r}, \underline{r}^1) dn(\underline{r}^1) U_0(\underline{r}^1) dV^1 \quad (2-7)$$

where G^0 is defined above.

Equations 2-4 and 2-7 represent "first order" solutions for the scattered field. They are "single scatter" solutions in that within the scattering medium, the incident field is always the free space field. The parabolic equation (2-6), on the other hand, can be used for "multiple scatter" or "strong scatter" conditions. In this report the emphasis is on the parabolic equation approach and, in particular, on the "thin phase screen" approximation to the parabolic equation to be derived later. For the sake of completeness, however, some results from the Born and Rytov approximations are included.

Section III - Second moment properties of the observed field
for various approximations.

The emphasis of this report is on displaying and explaining the second moment properties of fluctuations of the observed field as determined from scintillation measurements (observations of the "received signal", s - see glossary). These second moment properties can equivalently be presented in terms of covariance functions or spectral density functions.

For the Rytov approximations, we have

$$\psi_i = \psi - \psi_0 = \frac{k^2}{U_0} \int_V G^0 \, dn \, U_0 \, dV^1$$

while for the Born approximation:

$$\frac{U_i}{U_0} = \frac{U - U_0}{U_0} = \frac{k^2}{U_0} \int_V G^0 \, dn \, U_0 \, dV^1.$$

Thus the second moment properties, for example, of ψ_i and $\frac{U_i}{U_0}$ are identical in so far as the assumed approximations apply. As is shown later $R[\psi_i]$ is equated to the signal amplitude in db (i.e., log of A). Thus consider the Rytov approximation (2-7).

$$e^{\psi(\underline{r})} \equiv e^{\psi_0(\underline{r})} + \psi_i(\underline{r}) \equiv U_0(\underline{r}) e^{\psi_i(\underline{r})}$$

$$\psi_i(\underline{r}) \equiv x(\underline{r}) + iS(\underline{r}) = \int_V h(\underline{r}, \underline{r}^1) \, \delta n \, dV^1$$

where

$$h(\underline{r}, \underline{r}') = \frac{2k^2 G^0(\underline{r}, \underline{r}') U_0(\underline{r}')}{U_0(\underline{r})}$$

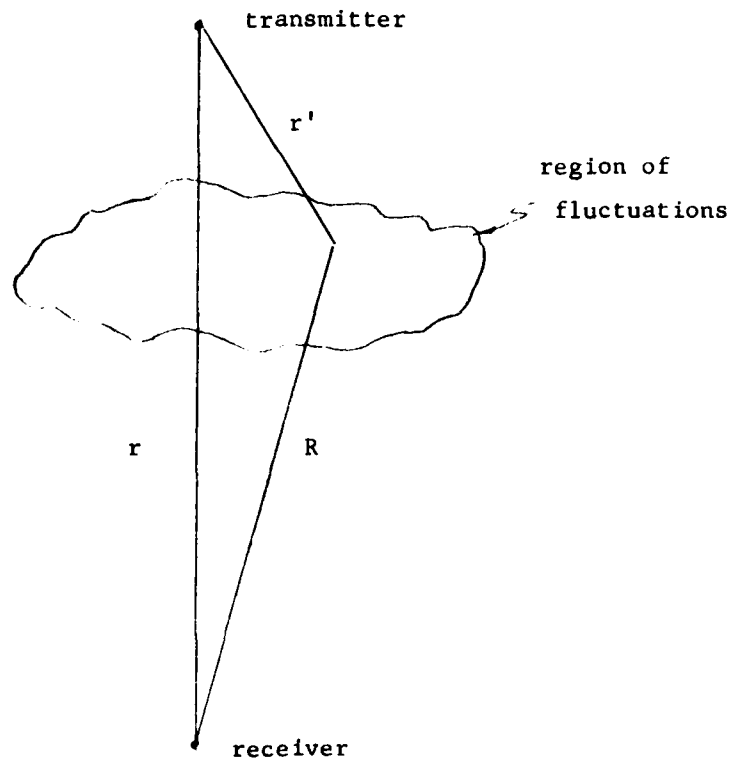
$$G^0(\underline{r}, \underline{r}') \equiv G^0(|\underline{r} - \underline{r}'|) = \frac{\exp(i k |\underline{r} - \underline{r}'|)}{4\pi |\underline{r} - \underline{r}'|}$$

The approximation

$$dn \equiv (1 + \delta n)^2 - 1 = 2\delta n + \delta n^2 \approx 2\delta n$$

has been used.

The following development (for a special geometry) is from Yeh and Lui (1972):



For a spherical wave

$$U_0(\underline{r}) = U_0(r) = \frac{A_0 \exp(i x r)}{r} \quad \text{where } r \equiv |\underline{r}|$$

and

$$k(\underline{r}, \underline{r}^1) = \frac{k^2}{2\pi} \frac{r}{R r_1} \exp[ik(R + r^1 - r)].$$

From this, obtain the following general expression for

$$B_X(\underline{r}_1, \underline{r}_2) = \langle X(\underline{r}_1) X(\underline{r}_2) \rangle = \frac{r_1 r_2}{(2\pi)^2} k^4 \cdot \int_{V_2} \int_{V_1} B_n(\underline{r}_1^1 - \underline{r}_2^1) \frac{\cos[k(R_1 + r_1^1 - r_1)]}{r_1^1 R_1} \cdot \frac{\cos[k(R_2 + r_2^1 - r_2)]}{r_2^1 R_2} dV_1^1 dV_2^1$$

where $B_n(\underline{r}_1^1 - \underline{r}_2^1)$ is the covariance function for the index of refraction fluctuations which is assumed to be a function of coordinate differences only. Note that \underline{r}_1 and \underline{r}_2 refer to coordinates at the observation points. A similar expression for B_S can be derived. This general expression can be greatly simplified for specific geometries.

and for the "forward scatter approximation" wherein the scale size of the fluctuations is much greater than λ . Thus consider the slab geometry shown in figure 2.

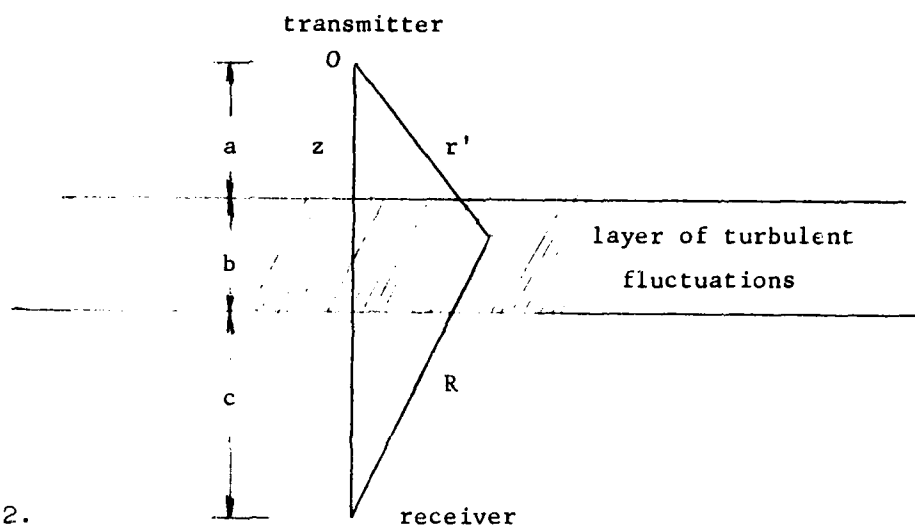


Figure 2.

From Yeh and Liu ([972]) B_X and B_S can be found from the following equations:

$$B_X(d, 0, L) = \frac{I_1 - I_2}{8\pi} ; B_S(d; L) = \frac{I_1 + I_2}{8\pi}$$

where

$$I_1 = \int_{z=a}^{a+b} \int_{z=-b}^b \int_{y=-\infty}^{\infty} \int_{x=-\infty}^{\infty} \frac{B_n(x, y, z)}{2z(1-2z/L)} \cdot$$

$$\sin \left[\frac{y^2 + (x+dZ/L)^2}{2z(1-2z/L)} \right] dx dy dz dZ$$

$$I_2 = \int_{z=a}^{a+b} \int_{z=-b}^b \int_{y=-\infty}^{\infty} \int_{x=-\infty}^{\infty} \frac{B_n(x, y, z)}{D + \frac{z^2}{L}} \cdot$$

$$\sin \left[\frac{y^2 + (x + dZ/L)^2}{D + \frac{z^2}{L}} \right] dx dy dz dZ$$

where $D = \frac{4Z(L-Z)}{L}$

This expression for B_x (and B_s) can be used for numerical computations for given B_n , or for simple forms of B_n and further simplifying assumptions some analytical expressions for the integrals may be obtained.

A similar geometry which allows for an angle of incidence γ of the (unperturbed) propagation direction w.r.t the slab normal is used in Taylor (1975) wherein relationships between the spectral density functions for x and n are derived under various simplifying assumptions and for incident plane waves.

Thus

$$\phi_X(\underline{\kappa}) = 2\pi k^2 \sec \gamma \int_0^d f(z) \sin^2 \left[\frac{L-z}{2k} (\kappa_X^2 \sec^2 \gamma + \kappa_y^2) \right] \cdot \phi_n(\kappa_x, \kappa_y, \kappa_x \tan \gamma) dz$$

where $f(z)$ is a function which takes account of a change of turbulence "levels" along the main propagation path. If the layer slant thickness, d , is such that $d \ll k l^2$ and $d \ll L$ where l is a mean scale size of the fluctuations, then

$$\phi_X(\underline{\kappa}) \sim \sin^2 \left[\frac{L}{2k} (\kappa_X^2 \sec^2 \gamma + \kappa_y^2) \right] \phi_S(\underline{\kappa})$$

where $\phi_S(\underline{\kappa})$ is the 2-dimensional phase fluctuation spectrum of the wave at the bottom of the slab. The same expression for intensity fluctuation spectra is derived in the next section indicating that under the assumptions used in the derivations log-amplitude spectra and intensity spectra are proportional. The function in braces is frequently referred to as the filter function. For the thin layer, this filter function is called the Fresnel filter.

Section IV - The thin phase screen approach

Starting with the parabolic equation (2-6), it is possible to make appropriate simplifications (for various geometries) and derive expressions for the spectrum of intensity fluctuations. In particular, the "thin phase-screen" or simply "thin screen" approximation can be derived. The net result is that the spectrum of electron density fluctuations (or equivalently, the spectrum of refractive index fluctuations) is multiplied by a filter function. The derivation of the \sin^2 filter was first done by Bowhill (1961) and later by Salpeter (1967) with results from Mercier (1962). The following is an outline of the "canonical" thin screen done essentially as in Ishimaru (1978).

Start with the parabolic equation (2-6) for $W(\underline{r})$ where the field is written as $U(\underline{r}) = W(\underline{r})e^{ikz}$ for forward propagation primarily in the z -direction. The intensity

fluctuations are derived from the fourth order moments of $W(\underline{r})$:

$$\Gamma_4 \equiv \langle W(z, \underline{\rho}_1) W(z, \underline{\rho}_2) W^*(z, \underline{\rho}_1^1) W^*(z, \underline{\rho}_2^1) \rangle$$

With an appropriate change of coordinates from the $\underline{\rho}_1, \underline{\rho}_2, \underline{\rho}_1^1, \underline{\rho}_2^1$ system to $\underline{R}, \underline{\rho}, \underline{r}_1, \underline{r}_2$ system, the parabolic equation for Γ_4 can be put into the form:

$$\left[\frac{d}{dz} - \frac{i}{k} \nabla_{\underline{s}_1} \cdot \nabla_{\underline{s}_2} Q \right] \Gamma_4 = 0$$

where

$$Q(\underline{s}_1, \underline{s}_2) = -\frac{kz}{2} [H(\underline{s}_1) + H(\underline{s}_2) - 1/2 H(\underline{s}_1 + \underline{s}_2) - 1/2 H(\underline{s}_1 - \underline{s}_2)]$$

$$H(\underline{\rho}) \equiv B_n(0) - B_n(\underline{\rho}).$$

$$\underline{R} = 1/4(\underline{\rho}_1 + \underline{\rho}_2 + \underline{\rho}_1^1 + \underline{\rho}_2^1)$$

$$\underline{\rho} = \underline{\rho}_1 + \underline{\rho}_2 - \underline{\rho}_1^1 - \underline{\rho}_2^1$$

$$\underline{s}_1 = 1/2(\underline{\rho}_1 - \underline{\rho}_2 + \underline{\rho}_1^1 - \underline{\rho}_2^1)$$

$$\underline{s}_2 = 1/2(\underline{\rho}_1 - \underline{\rho}_2 - \underline{\rho}_1^1 + \underline{\rho}_2^1).$$

Note that the implicit assumption has been made that only refractive index fluctuations in the plane perpendicular to the propagation direction are important in producing scintillation; thus B_n is a function of $\underline{\rho} \equiv (x, y)$ only.

The intensity fluctuations near a point z along the propagation path is $\Gamma_4(z, \underline{s}_1, 0)$.

The derivation of the expression for Γ_4 at a distance L from the front of a thin screen is done in two steps (plane waves are assumed - a correction for spherical waves is given later). First, the parabolic equation is integrated across the

thickness (Δz) of the screen. To first order, the result is that at the "bottom" of the screen ($z=0$)

$$\Gamma_4(0, \underline{s}_1, \underline{s}_2) = \exp(-Q(\underline{s}_1, \underline{s}_2), \Delta z)$$

(An alternative derivation for Γ_4 is to use the Rytov approximation to obtain an expression for Γ_4 at the "scintillation exit plane". See, for example, Tatarski (1961).)

The expression for Γ_4 at the receiver ($z=L$) can be obtained in various ways. The result is:

$$\Gamma_4(L, \underline{s}_1, \underline{s}_2) = \left(\frac{k}{2\pi L}\right)^2 \int_{-\infty}^{\infty} d\underline{s}_1^i d\underline{s}_1^j \exp\left[\frac{ik}{L}(\underline{s}_1 - \underline{s}_1^i) \cdot (\underline{s}_2 - \underline{s}_2^i) + \Delta Q(\underline{s}_1^i, \underline{s}_2^i)\right]$$

Alternatively, $\Gamma_4(L, \underline{s}_1, \underline{s}_2)$ can be written as

$$\Gamma_4(L, \underline{s}_1, \underline{s}_2) = \int_{-\infty}^{\infty} S(L, \underline{\kappa}, \underline{s}_2) e^{i\underline{\kappa} \cdot \underline{s}_1} d\underline{\kappa}$$

where

$$S(L, \underline{\kappa}, \underline{s}_2) = \frac{1}{(2\pi)^2} \int e^{-i\underline{\kappa} \cdot \underline{s}_1^i + \Delta Q(\underline{s}_1^i, \underline{s}_2 - \frac{\underline{\kappa} L}{k})} d\underline{s}_1^i.$$

Note that $S(L, \underline{\kappa}, 0) = \hat{\Gamma}_4(L, \underline{s}_1, 0)$ is the spectral density function for intensity scintillations and is essentially the quantity which is measured.

By making further approximations, it is possible to derive various "filter functions" which associate the scintillation spectrum at the observation point ($z=L$) to that at the phase screen. For example, if the first order approximation $e^Q \sim 1+Q$ as used by Salpeter (1967) is made, the \sin^2 filter function is found. Thus:

$$S(L, \underline{\kappa}, \phi) \sim \frac{1}{(2\pi)^2} \int [1 + \Delta Q(\underline{s}_1, -\frac{\underline{\kappa}L}{k})] e^{-i\underline{\kappa} \cdot \underline{s}_1} d\underline{s}_1 =$$

$$\frac{1}{(2\pi)^2} \int [1 - \frac{\Delta k^2}{2} H(\frac{-\underline{\kappa}L}{k})] e^{-i\underline{\kappa} \cdot \underline{s}_1} d\underline{s}_1$$

$$- \frac{k^2}{2(2\pi)^2} \Delta \int [H(\underline{s}_1) - 1/2H(\underline{s}_1 - \frac{\underline{\kappa}L}{k}) - 1/2H(\underline{s}_1 + \frac{\underline{\kappa}L}{k})] e^{-i\underline{\kappa} \cdot \underline{s}_1} d\underline{s}_1.$$

The first term gives rise to a "delta" function which is unimportant for the study of scintillation spectra. The second term can be written as:

$$- \frac{k^2}{2} \Delta \hat{H}(\underline{\kappa}) [1 - \frac{(e^{2i|\underline{\kappa}|^2 L / 2k} + e^{-2i|\underline{\kappa}|^2 L / 2k})}{2}]$$

$$= - \frac{k^2}{2} \Delta \hat{H}(\underline{\kappa}) \sin^2(\frac{|\underline{\kappa}|^2 L}{2k})$$

where $|\underline{\kappa}|^2 = x^2 + y^2$

and $\hat{H}(\underline{\kappa})$ is the Fourier transform of H and is essentially the (2-dimensional) spectrum of the refractive index fluctuations. Thus:

$$S_I(L, \underline{\kappa}) \equiv S(L, \underline{\kappa}, 0) = C(k) S_N(\underline{\kappa}) \sin^2(\frac{|\underline{\kappa}|^2 L}{2k})$$

where C is a constant which depends on the free space wave number k and some geometric quantities.

The above derivation assumes a plane wave incident on the fluctuation slab and, in addition, that the propagation path is normal to the slab. Two corrections must be made for spherical waves and/or non-normality.

(a) spherical wave correction - Ishimaru (1978)

$\underline{\kappa} \rightarrow \frac{L_1 + L_2}{L_1} \underline{\kappa}$ where L_1 is the distance from source to slab and L_2 is the distance from slab to receiver.

(b) the angle between the propagation path and slab normal is γ . The propagation path is in the x-z plane - Taylor (1975). $\kappa_x \rightarrow \kappa_x \sec \gamma$

$L \rightarrow$ slant distance.

Section V - A choice of approaches

As shown above, the Rytov and thin screen approximations give basically the same results for a thin slab of fluctuations. There is good evidence that the thin slab approach is applicable for radio waves traversing the ionosphere wherein the slab is located near the electron density peak. In any case, a choice has to be made and at least for a first approximation to the truth, it is used here. Specifically, the results derived in Taylor (1975) for a uniform slab are used:

$$\text{let } \kappa_c^2 = \kappa_x^2 \sec \gamma + \kappa_y^2$$

then

$$\Phi(\underline{\kappa}) = \pi k^2 d \sec \gamma \left\{ 1 + \frac{k}{d \kappa_c^2} \left[\sin\left(\frac{L-d}{k} \cdot \kappa_c^2\right) - \sin\left(\frac{L}{k} \cdot \kappa_c^2\right) \right] \right\} \Phi_n(\kappa_x, \kappa_y, \kappa_x \tan \gamma)$$

For equatorial scintillation, Φ_n is highly anisotropic. Taylor (1975) derives some useful expressions under the assumption that the correlation function for anisotropic fluctuations is obtained directly from that for isotropic fluctuations by a scale multiplication. The final results are:

$$\Phi_n(\kappa_x, \kappa_y, \kappa_z \tan \gamma) = a \Phi_n^i \{ a^2 [\kappa_x (\cos \phi \cos \theta - \sin \theta \tan \gamma) + \kappa_y \sin \phi \cos \theta]^2 + (-\kappa_x \sin \phi + \kappa_y \cos \phi)^2 + [\kappa_x (\cos \phi \sin \theta + \cos \theta \tan \gamma) + \kappa_y \sin \phi \sin \theta]^2 \}^{1/2} .$$

where:

$\Phi_n^i(\underline{\kappa})$ is the spectral density function for the "associated" isotropic fluctuation.

a is the "elongation factor" for the anisotropic fluctuation correlation function. (Typically, imagine correlation ellipsoids of revolution. Then a is the ratio of the major and minor axes.)

ϕ is the angle the major axis plane makes with the observation plane.

θ is the angle the major axis makes with the x, y plane.

The last step is the relationship between $\Phi_\chi(\underline{\kappa})$, the spatial spectral density function and $S_\chi(\omega)$, the temporal (observed) spectral density function. Taylor's (1938) hypothesis of "frozen" turbulence is used to make the transition (see Wyngaard and Clifford (1977) for a discussion of the validity of this hypothesis). The approximation amounts to performing the steps:

$$(1) F(K_\chi) = \int_{-\infty}^{\infty} \Phi(\underline{K}) dK_y, dK_z \quad (\text{for the general 3D case}).$$

$$(2) S(\omega) = \frac{1}{v} F\left(\frac{\omega}{v}\right) \text{ where the "irregularities" drift in the } x\text{-direction with speed } v.$$

This approximation assumes that the x -direction can be freely chosen. However, for the geometry considered here, the coordinate system has been fixed by the vertical plane through the slant line joining transmitter and receiver and the local vertical.

Thus the following transformations must be made:

(1) $\phi_X(\kappa_X, \kappa_Y) \rightarrow \phi_X(\kappa_X^1, \kappa_Y^1)$ by the substitution

$$\kappa_X = \kappa_X^1 \cos \alpha - \kappa_Y^1 \sin \alpha$$

$$\kappa_Y = \kappa_X^1 \sin \alpha + \kappa_Y^1 \cos \alpha$$

where the drift direction is along the x^1 axis which makes an angle α with the x -axis.

$$(2) F(\kappa_X^1) = \int_{-\infty}^{\infty} \phi_X(\kappa_X^1, \kappa_Y^1) d\kappa_Y^1$$

$$(3) S(\omega) = \frac{1}{v} F\left(\frac{\omega}{v}\right)$$

Section VI - Examples

The model presented above contains many parameters which are listed below.

- (1) general parameters which define the isotropic refractive index spectral density function. For example, l_0 and L_0 for the Kolmogorov spectrum.
- (2) d , the slab slant thickness.
- (3) L , the slant range to the top of the slab from the receiver.
- (4) the velocity of the slab relative to the slant mean propagation path. This consists of two parameters, v and α .
- (5) the parameters a, θ and ϕ which describe the anisotropy of the index of refraction fluctuations relative to the coordinate system defined by the slant path.

The coordinate system defined by the slant path changes in time due to motion of the transmitter and receiver. In addition, of course, the fluctuation slab is assumed to move relative to the slant path. (The condition $v=0$ can presumably occur, in which case, the scintillation spectrum S is not defined.) During a given observation of S , it is assumed that all parameters remain constant. A computer subroutine has been written (see Appendix A) which provides the parameters v and α given the satellite (orbital parameters $X, Y, Z, \dot{X}, \dot{Y}, \dot{Z}$), the aircraft position and

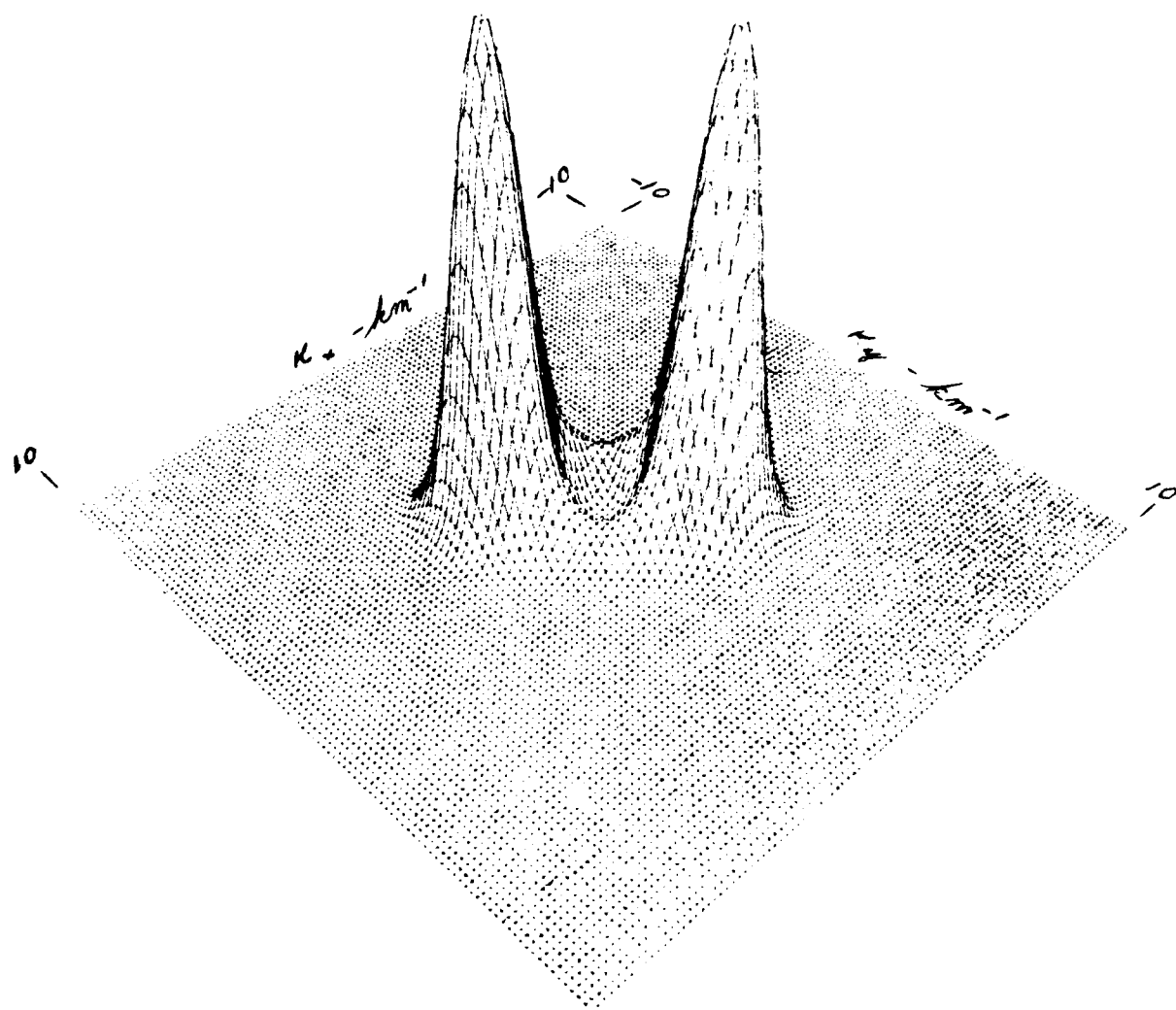
velocity vector for the mean slab motion (relative to a fixed earth). Various spectra have been computed using the above models with various values for the parameters. In particular, these calculations have been done for Gaussian, power law and Kolmogorov (or von Karman) spectra.

Figures 3a, b, c show the function $\psi_x(\kappa_x, \kappa_y)$ for

- a) ψ_n Gaussian
- b) ψ_n power law
- c) ψ_n von Karman

The following parameter values for ψ_x were used:

transmitter frequency	100MHz
slant angle (γ)	0°
distance from layer to receiver (L)	300km
layer thickness (D)	10km
correlation "ellipsoid" values:	
(a)	2.
(θ)	25 deg.
(ϕ)	45 deg.

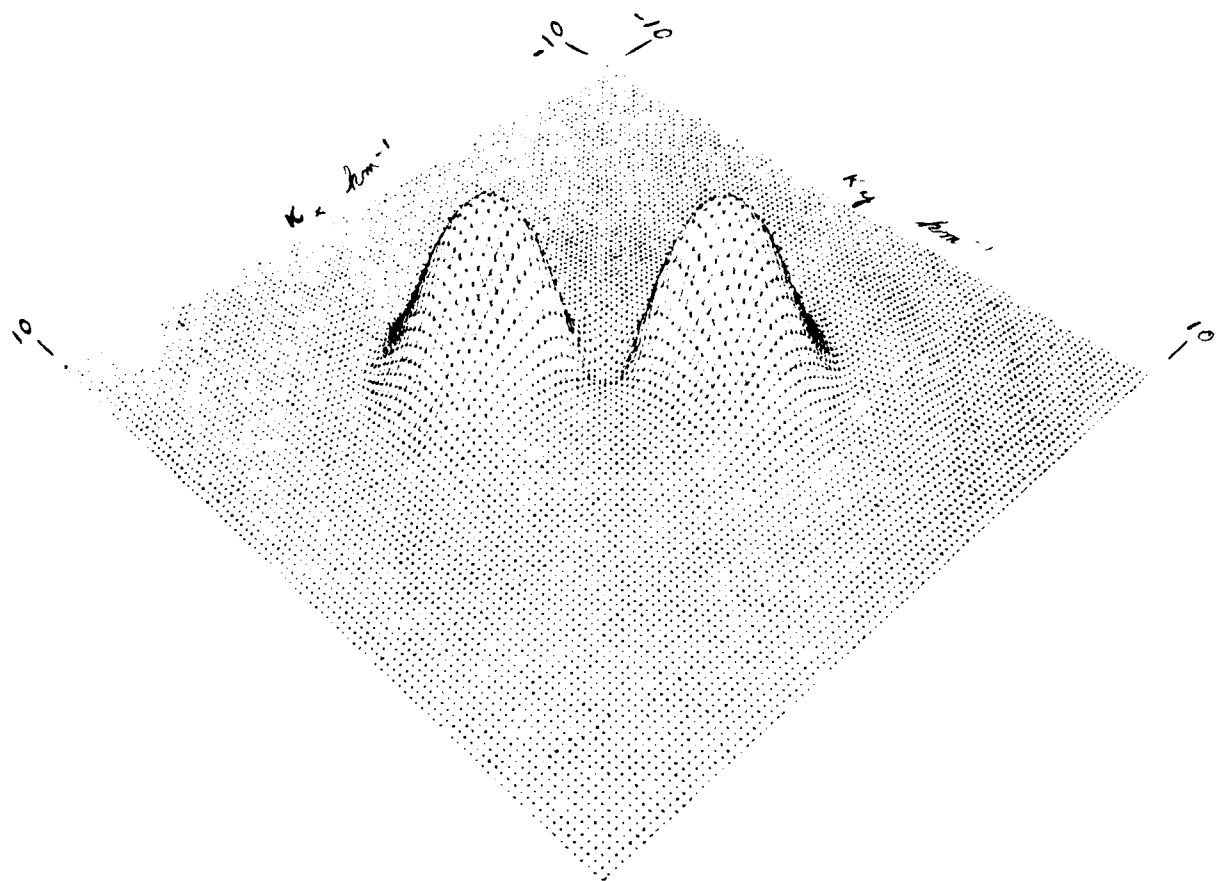


ϕ_x - Gaussian ϕ_n

$$\phi_n = \frac{p^{3/8}}{\pi \sqrt{\pi}} \exp(-x^2 p^2 / 4)$$

$$p_1 = p = 1$$

Figure 3a.

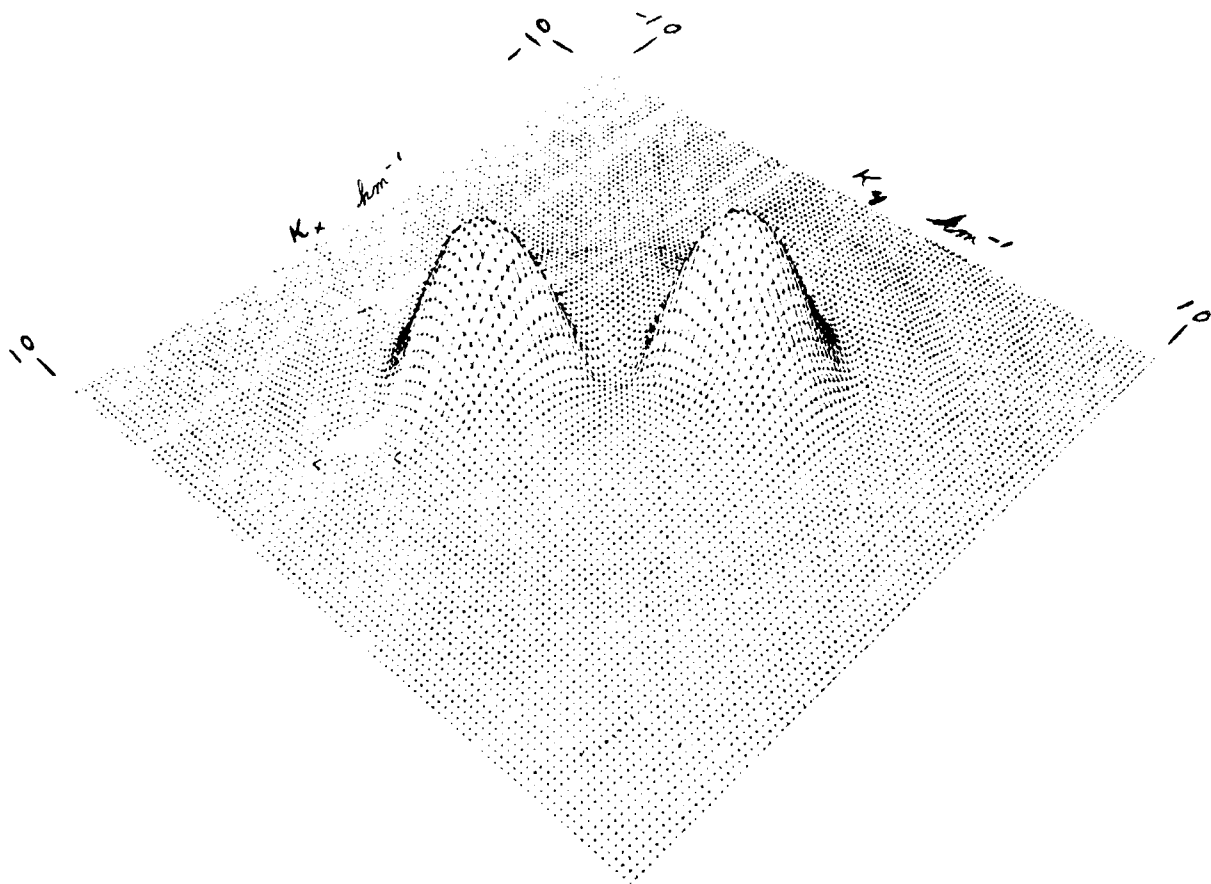


ϕ_x - power law ϕ_n

$$\phi_n = \left(\frac{p^d}{\pi^2}\right) \cdot \frac{1}{(1+x^2 p^2)^2}$$

$$p_1 = p = 1$$

Figure 3b.



ϕ_x - von Karman ϕ_n

$$\phi_n = .063 p^{-2/3} \left(x^2 + \frac{1}{p^2} \right)^{-11/6} \exp(-x^2 q^2)$$

$$p_1 = p = 1 \quad q = .000169 \quad (q = p_2 / .00592)$$

Figure 3c.

It should be noted that all of the physics of this particular model of amplitude scintillation is contained in these functions, $\Phi_X(\kappa_X, \kappa_Y)$. The amplitude spectra are obtained from these functions by first rotating the κ -coordinate frame over which they are defined by angle α and then integrating from $-\infty$ to ∞ the resulting function in the κ_Y^\perp direction for all values of κ_X^\perp . Because of symmetry, values of $\kappa_X^\perp \geq 0$, only, need be considered. The final "transformation" from $\Phi_X(\kappa_X, \kappa_Y)$ to $S(\omega)$ is merely one of stretching or compression and normalization such that the area under the function remains the same. Thus it is important to study the structure of these functions in both a qualitative and quantitative manner. The transformations mentioned above can be done mentally in a qualitative fashion using the illustrated functions as examples of Φ_X . In this report, the structure of Φ_X is not investigated.

In Figure 4, which is a plot of the function $S(f) = S(\frac{\omega}{2\pi})$, some examples are shown of the above transformations of a single Φ_X for an actual aircraft/satellite geometry (as occurred on October 20, 1976). This figure is an illustration of the output of a set of computer software designed for comparing theoretical and experimental spectra. Again, it is not the intent of this report to delve into the structure of the spectra. Appendices A and B provide some information on the algorithms used in producing Figure 4.

The following fixed parameters were used:

satellite	- LES9
transmitter freq.	- 249 MHz
date/time	- 76/10/20/1/8/0
A/C height	- 30000 ft.
A/C location	- lat -11°, long -77°
A/C speed	- 470 knots
layer model	- power law (p=3)
layer speed	- 70 m/s
layer direction	- 90° (geographic east)
layer "shape"	- $\theta = 0^\circ$, $\phi = 0^\circ$, $a = 10$
layer thickness	- 10 km

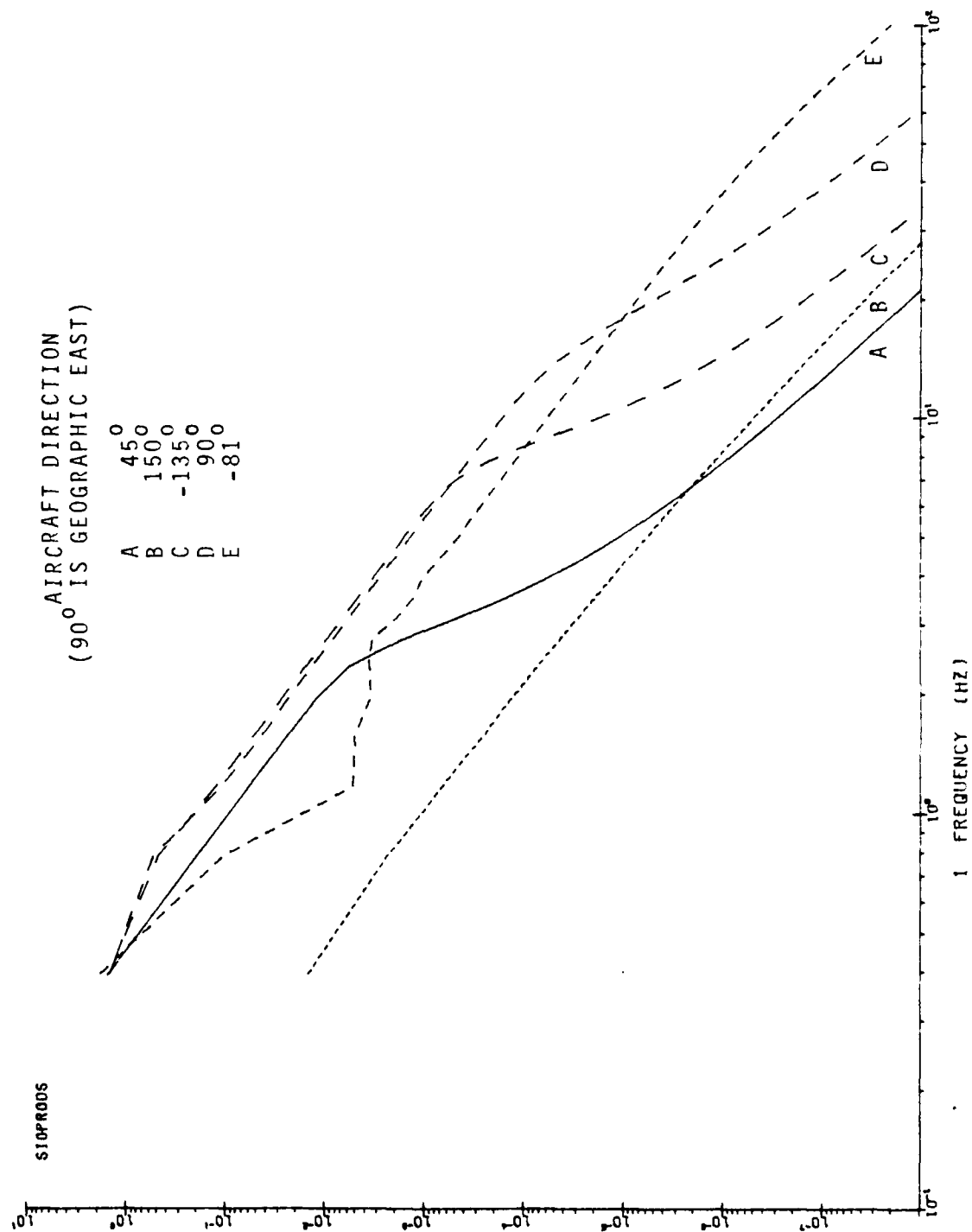


Figure 4 - Theoretical $S(f) = S(-\frac{\omega}{2\pi})$ for various aircraft directions (see preceding page for other parameter values)

Section VII

In this section a brief overview of "spectral analysis" is presented along with a description of the actual spectral analysis technique used to compare theory with experiment.

The theoretical quantity of interest is the "measurable" scintillation spectral density function, $S(\omega)$, related as shown previously to the spectral density function of electron density fluctuations. The function $S(\omega)$ is presumably well defined and measurable (or more exactly determinable) over a portion of the frequency domain $-\infty$ to $+\infty$. Because the underlying stochastic process is real, $S(\omega)$ is even and need be determined only over 0 to ∞ . Moreover, $S(\omega)$, for all practical purposes, is negligible beyond some ω which can be determined from the model parameters as listed in the previous section. $S(\omega)$ is, of course, a probabilistic concept, summarizing some (and perhaps all) of the second moment properties of an underlying stationary stochastic process. The task at hand is to estimate $S(\omega)$ or perhaps a portion of $S(\omega)$ given a finite (and relatively small) observation (or "realization") of the process.

Thus we enter the broad expanse of another discipline called spectrum (or spectral) analysis or more exactly (but verbose), the theory and practice of estimating a spectral density function of a (in general) "homogeneous process" given one or more finite realizations of this process. The term "homogeneous process" is put in quotes because quite often it is not clear that the underlying model is a homogeneous process (e.g., to what extent is human speech a homogeneous process), and modern spectral analysis is not limited to homogeneous (or stationary) processes although it often is not clear how the spectrum should be defined for "non-homogeneous" processes. None-the-less, it is quite clear in this study of scintillation spectral analysis, the process behind the $S(\omega)$ is (assumed to be) stationary. (Note that the term homogeneous usually is reserved for stochastic processes defined in space while stationary is reserved for "random signals", i.e., "random functions of time".)

The underlying process (random signal or whatever one wants to call it) is an observed AVC voltage which can, by suitable transformations, be made proportional to the scintillation amplitude A as defined in the glossary. Note that synchronous detection is not used here so that the X and Y components of the signal cannot be

determined separately. In addition to being of finite duration, the process is digitized either directly during the recording process (after Jan. 1979) or prior to analysis. (Prior to 1979, the signal voltage was recorded directly on an FM magnetic tape recorder and later digitized prior to analysis). Thus the underlying process can better be thought of as a "time series" and the usual techniques of time series spectrum analysis can be applied.

Before delving into the subject of time series spectrum analysis, it is worthwhile to bridge the gap between the "continuous domain" and the "discrete domain" brought about by sampling and to then forget entirely about the continuous domain (it remains tied to the discrete domain through some frequency conversion constants and assumptions on the "band width" of the original signal).

First of all it is assumed that the sample interval Δt (assumed constant) is always such that the Nyquist criteria is met, i.e., $\Delta t \leq \pi/\omega_c$ where ω_c is such that $S(\omega) = 0$ for $|\omega| > \omega_c$. In practice, this condition is better stated as "the sample interval is small enough such that spectral aliasing is negligible." Unfortunately this condition may sometimes be inadvertently violated. For example, unknown high frequency noise may be present in the observing system. Violation of this condition can frequently be detected by estimating the spectrum at various sample intervals.

Once in the "discrete domain" it is convenient to use a unit sample interval (basically a time series is a random function over the integers (usually represented in group theory, at least, by Z)). The spectral density functions which might be defined for such time series is defined over $-\pi \leq \omega \leq \pi$ (more exactly $S(\omega)$ is periodic with period 2π). The estimated spectral density functions which are defined over $[-\pi, \pi]$ can be associated with the original (unsampled) process by using the conversion factor $\frac{1}{\Delta t}$, i.e., $S(\omega) \rightarrow S(\frac{\omega}{\Delta t})$. In particular, given the sample interval Δt , the spectrum can only be estimated up to a (radial) frequency given by $\frac{\pi}{\omega t}$ (or up to $\frac{1}{2\Delta t}$ Hertz). It is intuitively obvious perhaps that the sample size, N , (the original observation now consists of N signal values x_0, x_1, \dots, x_{N-1}) limits the low end of the spectrum or, more exactly, essentially limits the accuracy of estimating the spectrum near $\omega = 0$. [This is usually not a problem since one usually

is not interested nor should be interested in $S(\omega)$ at $\omega = 0$.] Roughly speaking, the lower limiting (radial) frequency for a reliable estimate of $S(\omega)$ is $\omega = \frac{\pi}{M\Delta t}$ where $M < N$ is a "truncation" number used to reduce the variance in the estimate of S . (Because of the previously mentioned evenness of $S(\omega)$ it is only necessary to discuss estimating S for positive frequencies.)

Historically, spectral analysis of time series really got its main "modern" impetus with the publication in 1959 of "The Measurement of Power Spectra", Blackman and Tukey (1959). During the decade of the 60's the theory and technique of spectral analysis became the subject of many articles and books. During this period, the subject arrived at its "classical formulation" which is still the one most often used. (It is quite adequate for many purposes.) A good summary of this formulation can be found in Koopmans (1974).

During the last decade, more "powerful" techniques of spectral analysis have become more common place. These methods are usually referred to as the MEM or MLM methods (for maximum entropy method and maximum likelihood method, respectively). These (currently modern) methods as well as the "classical" methods of spectral analysis are summarized in a collection of reprints by Childers (1978). The Proceedings of the RADC Spectrum Estimation Workshop (1978) also contains several up-to-date "working" methods for spectrum analysis and provides an overview of many diverse areas where spectral analysis is used. A fairly recent article which gives the "modern flavor" of spectral analysis can be found in Thomson (1977).

Before giving the particular algorithm which is used here for estimating $S(\omega)$ from the observed time series, it is worthwhile to first quickly review some of the primary ideas which led to the development of the algorithm which, by the way, is approximately equivalent to most other "classical" methods.

First of all, the whole idea of associating a "spectrum" with a time series is an attempt to "Fourier analyze" (or harmonic analyze) observed data - to break it down into its fundamental components, so to speak. Mathematically, the problem is one of generalizing the concept of Fourier series or the Fourier integral for finite "energy functions". This generalization can be approached from two directions, i.e., through probability theory (stationary stochastic processes) or finite "power"

but "deterministic" functions. (From a practical standpoint, there is little obvious difference between a (segment of) a deterministic waveform and a (segment of) a realization of a stochastic waveform. The main difference is that with the latter one can associate various probabilities and "expected values", while with the former this cannot be done, at least not with the same interpretations.) The approach to spectral analysis via stochastic process theory is less intuitive than that through finite power function theory so we choose the latter to start with but soon switch over to results from stochastic process theory. This approach also has the advantage that the rationale behind the spectrum estimation algorithm is somewhat more obvious.

To start with, consider the class of real or complex valued functions on Z (the integers) such that

$$(7.1) \quad \phi(n) = \lim_{N \rightarrow \infty} \frac{1}{2N+1} \sum_{n'=-N}^N f(n')f(n'+n)$$

exist for all $n \in Z$.

(This class is the discrete analog of "finite power" signals $f(t)$ such that

$$\phi(t) = \lim_{T \rightarrow \infty} \frac{1}{2T} \int_{-T}^T f(t')f(t'+t)dt'$$

exists and is non-trivial for all $t \in R$. Since we deal only with "digitized" wave forms, it is simpler to consider functions defined over Z to begin with but to keep in mind the sample interval Δ and the specter of possible aliasing.) $\phi(n)$ is called the "autocorrelation function of f ". Functions of this class were first seriously considered by Norbert Wiener. They are not amenable to harmonic analysis in the usual sense although it is possible to develop a "generalized" harmonic analysis for such functions which is very similar to that which has been developed for stochastic processes. The function $\phi(n)$ is positive definite and can always be represented in the form

$\phi(n) = \int_{-\pi}^{\pi} e^{in\omega} dF(\omega)$ and if F is absolutely continuous,

$\phi(n) = \int_{-\pi}^{\pi} s(\omega) e^{in\omega} d\omega$. Furthermore, assuming the inverse

Fourier transform exists,

$$(7.2) \quad s(\omega) = \frac{1}{2\pi} \sum_{n \in \mathbb{Z}} \phi(n) e^{-in\omega}.$$

The function $s(\omega)$ is frequently called the spectral density function of f ; it is the functional analog of $S(\omega)$, the spectral density function associated with a stationary stochastic sequence (or time series).

Non-trivial examples of f with a given associated s can be constructed using "Wiener numbers", see Papoulis (1962) as input to a digital filter with amplitude response $|H(\omega)|$ such that $|H(\omega)|^2 = s(\omega)$.

Consider next the problem of determining (or estimating $s(\omega)$) given $f(n)$ on $[0, N]$ or $[-N, N]$. More explicitly, consider a sequence of (in this case, real valued) functions $f_N(n)$ on \mathbb{Z} which are identically zero for $|n| > N$ and such that $f_N(n) = f(n)$ for $|n| \leq N$. For each such f_N consider the quantity

$$(7.3) \quad s_N(\omega) = \frac{1}{2\pi} \frac{1}{2N+1} \left| \sum_{n \in \mathbb{Z}} f_N(n) e^{-in\omega} \right|^2.$$

Using results from Fourier analysis, it is easy to show that

$$(7.4) \quad s_N(\omega) = \frac{1}{2\pi} \sum_{n=-2N}^{2N} \phi_N(n) e^{-in\omega}$$

where

$$\phi_N(n) = \frac{1}{2N+1} f_N^* f_N(n) \quad (\text{where } * = \text{correlation})$$

$$\text{i.e., in general, } f^* g(n) = \sum_{n' \in \mathbb{Z}} \bar{f}(n') g(n+n') \text{ for}$$

complex valued f, g and $\bar{}$ means conjugation.

Comparing equations (7.4) and (7.2), it seems plausible that $s(\omega)$ can be "estimated" by

$$(7.5) \quad \frac{1}{2\pi} \frac{1}{2N+1} \left| \sum_{n=-N}^N f_N(n) e^{-in\omega} \right|^2 \text{ for some suitably large } N.$$

We now turn immediately to the completely analogous situation where instead of a (deterministic) function f , we have a time series (realization of a stationary stochastic sequence), specifically N values of the time series and define the analog of equation (7.5).

$$(7.6) \quad I_N(\omega) = \frac{1}{2\pi N} \left| \sum_{n=1}^N x_N(n) e^{-in\omega} \right|^2$$

(Here the time series x is, for historical reasons, indexed from 1 to N rather than from $-N$ to N .)

$$= \frac{1}{2\pi} \sum_{n=-N+1}^{N-1} R_N(n) e^{-in\omega}$$

$$\text{where } R_N(n) = R_N(-n) = \frac{1}{N} x_N^* x_N(n) = \frac{1}{N} \sum_{n'=1}^{N-1} x_N(n') x_N(n'+n)$$

$$= \frac{1}{N} \sum_{n'=1}^{N-n} x(n') x(n'+n)$$

where $x_N(n) = x(n)$, $n=1, \dots, N$; $x_N(n)=0$ elsewhere.

I_N is called the "periodogram" and R_N the correlogram associated with the time series. They are the basis for most of "classical" spectral analysis.

It can be shown, see for example Hannan (1967), that I_N is not a "consistent" estimator of $S(\omega)$ associated with the time series. That is, the variance of I_N does not approach zero as the length, N , of the time series goes to ∞ (although the expected value of $I_N(\omega)$ approaches $S(\omega)$). In fact, at least for a Gaussian time series

$$\text{var}[I_N(\omega)] \longrightarrow \sigma^4 S^2(\omega)$$

where σ^2 is the variance of x . (Unless noted otherwise, it is assumed that x has mean zero.)

Faced with this "inconsistency" dilemma, the most obvious solution is to somehow obtain an "average" periodogram in the hope that the "fluctuations" in the estimator (as measured by the variance of the estimator) will approach zero for large N . In fact, the art of spectral analysis (specifically the art of spectral density function estimation) was initiated by Bartlett (1950) when he published results of a careful analysis of this averaging process. Briefly, the averaging is done by breaking the time series of length N into M segments of equal length N' , compute the periodogram for each segment, and then average them. Without going into the details, it can be shown that this process is equivalent to estimating $S(\omega)$ by

$$S_N^B(\omega) = \frac{1}{2\pi} \sum_{n=-N'+1}^{N'-1} w_N(n) R_N(n) e^{-in\omega}$$

where $w_N(n) = 1 - |n|/N'$ $-N' \leq n \leq N'$
 $= 0$ elsewhere

and $N = MN'$

The variance of S_N^B , ($\text{var}[S_N^B(\omega)]$), is given by

$$\text{var}[S_N^B(\omega)] = \text{var}[I_N(\omega)]/M.$$

Thus assuming that M becomes large with N , S_N^B is a consistent estimator. The next logical step is to introduce a general estimator of the form

$$\begin{aligned} (7.7) \quad S_N(\omega) &= \frac{1}{2\pi} \sum_{n=-m_T+1}^{m_T-1} w(n) R_N(n) e^{-in\omega} \\ &= \frac{1}{2\pi} \sum_{n \in Z} w_N(n) R_N(n) e^{-in\omega} \end{aligned}$$

where w_N is defined to be zero for $|n| > N$. The integer m_T is referred to as the "truncation point" and the function w_N is called the "lag window".

A further generalization is developed in Grenander and Rosenblatt (1957) where the estimator

$$S_N(\omega) = \frac{1}{2\pi N} \sum_{n, n'}^N b_N(n, n') x(n) x(n') \text{ is analyzed.}$$

The $b_N(n, n') = b_N(n', n)$ is a set (indexed by N) of real valued functions on $Z \times Z$. Furthermore, if $b_N(n, n')$ is chosen such that

$$b_N(n, n') = \int_{-\pi}^{\pi} V_N(y) e^{i(n-n')y} dy$$

where V_N is a real or complex valued function with a Fourier transform, then one obtains essentially an estimate of the form given by equation (7.6). Estimates of this type are called spectrogram estimates. If v_N (the Fourier transform of V_N) is identically zero for $|n| > m_T - 1$, then $S_N(\omega)$ is called a truncated spectrograph estimate.

One advantage of spectrograph estimates (as a class) is that their statistical properties are quite well understood. There are several other "classical" methods of spectral analysis which are not strictly of the spectrograph type. For example, a common method is to divide the time series of length N into M segments which generally overlap. A suitable real weight function (or "fader"), $a(n)$, is chosen and the quantity

$$z_l(j) = \sum_{n=0}^{2m-1} a(n)x_l(n)e^{i\frac{2\pi nj}{2m}}$$

$j=0, \dots, m$ is found for each segment l where $2m$ is the length of each segment.

The quantities $|z_l(j)|^2$ are then averaged to provide estimates of $S_N(\omega)$ for

$$\omega = \frac{2\pi j}{2m}$$

In this method the data itself is "windowed" rather than the correlogram.

It should be pointed out here that all of the "classical" methods are "ad hoc" in the sense that an estimator (or estimation method) is proposed (e.g., the general spectrograph estimator) and then some of its statistical and other properties are investigated. All of them include a "window function" of some sort and much has been written about the properties of various windows. Also these methods share the common practice of appending zeros to the data (or the correlogram), a practice which can be paraphrased as observer introduced "bias" to the data. Arbitrary windowing and adding zeros are both practices which is tantamount to the user inserting "information" in the estimating procedure - information which has no basis in fact. The introduction to the modern era of spectral analysis is aptly summarized by Ables (1978) wherein any data reduction method (including spectral analysis) should be "consistent with all relevant data and maximally non-committal with regard to unavailable data" (roughly speaking, a maximum entropy principle). Unfortunately, this principle which is so appealing and easy to state does not provide for a method of spectral analysis; one still must devise a method which "works" in some sense and then see if it follows the maximum entropy principle.

For the task at hand, we do not really want to compute the spectrum per se, but to do some hypothesis testing, e.g., test the hypothesis that the observed spectrum is due to a power law electron density spectrum against the alternative hypothesis of a Gaussian electron density spectrum, etc. Never-the-less, in this report, the hypothesis testing approach is not used from "first principles". Rather theoretical spectra and experimental spectra are derived and compared in the obvious manner. Moreover, for reasons of expediency, the classical (truncated) spectrograph estimator is used. Details of the estimator (estimation method) are given in Appendix C.

This section on spectral analysis is completed by presenting some well known properties of spectrograph estimators (derivations and more details can be found in Koopmans (1974)).

(1) Confidence region

If it is possible to derive a probability distribution function for a given estimator $S_N(\omega)$ and to do this for all ω , ($0 \leq \omega \leq \pi$), then calculated estimates can be placed within a confidence region or more exactly a confidence region can be superimposed on a set of estimates $S_N^*(\omega)$ (note that a generic estimator (actually a random function) is denoted by $S_N(\omega)$, while a specific estimate is, here, denoted by $S_N^*(\omega)$). It is then possible to make the pseudo-mathematical statement that "with P% confidence, the true value of $S(\omega)$ is within the given region" (which depends among other things on $S^*(\omega)$ itself).

Approximately, it can be shown (see, for example, Koopmans (1974) or Jenkins and Watts (1968) that the probability distribution for $\frac{S_N(\omega)}{S(\omega)}$ is given by $P(\chi^2 | \nu)$ where $P(\chi^2 | \nu)$ is the chi-squared distribution for ν -degrees of freedom and ν is given by

$$\nu = \frac{2N}{\pi T \|h\|_2^2} \quad (\nu \text{ is half the above value at the ends } (0, \pi) \text{ of the interval})$$

where $\|h\|_2 = [\int_{-1}^1 h^2(t) dt]^{1/2}$ is the norm of the window function referred to previously. (It is customary to define the various window functions such that $w_N(n) = h(\frac{n}{N})$ where h is defined on \mathbb{R} with support $[-1, 1]$.)

It is convenient to display $\log S_N^*(\omega)$ rather than $S_N^*(\omega)$ since the length of the confidence interval for $\log S(\omega)$ is independent of ω . The $100(1-\alpha)\%$ confidence interval is

$$[\log(\frac{a}{b}) + \log S_N^*(\omega), \log(\frac{a}{b}) + \log S_N^*(\omega)]$$

where a and b are such that

$$P(u \leq a) = \frac{\alpha}{2},$$

$$P(u \leq b) = 1 - \frac{\alpha}{2}$$

From this it follows that $\log \frac{b}{a}$ is the constant length of the confidence interval on a log scale.

In deriving the above results, several assumptions are made but which are not strictly true. For example, it is assumed that the bias of the estimator (see next sub-section) is zero; it is also assumed that the estimates at the various ω values are uncorrelated (also see below). Actually estimates are approximately uncorrelated only at

$$\omega = \omega_k = \frac{2\pi k}{mT} \text{ for } k = 0, \dots, mT/2.$$

(2) Bias

The bias of an estimator is a measure of how "closely" the estimator can, in the limit, estimate. This measure is

$$B_N(u) = E S_N(\omega) - S(\omega) \quad (E \text{ means expectation})$$

It is usually difficult to find useful expressions for bias and they frequently depend on derivatives of $S(\omega)$ which are unknown (since $S(\omega)$ is unknown). For example, for the window function used in this report

$$B_N(\omega) \approx \frac{6}{m^2 T} S''(\omega) \quad (" \text{ means second derivative})$$

A very important consequence of bias (which usually can be ignored for relatively smooth spectra) is the inaccuracies it produces when the observations (the time series) have non-zero mean. In fact, if the mean of the series is large compared with its variance, bias will cause the estimator to behave like $(1-\cos\omega)^{-1}$ for all ω regardless of the true shape of $S(\omega)$.

(3) Variance

Like bias, it is difficult to obtain an "exact" expression for the variance of an estimator. An approximate form (which follows from the chi-squared probability distribution for $S_N(\omega)$) is

$$\begin{aligned} \text{var}[S_N(\omega)] &\approx \frac{2mT}{N} S^2(\omega) \|h\|_2^2 \quad \omega = 0, \pi \\ &\approx \frac{mT}{N} S^2(\omega) \|h\|_2^2 \quad \omega \neq 0, \pi \end{aligned}$$

(4) Correlation

The covariance of two random variables is an important parameter since non-zero covariance at least indicates that the random variables cannot be independent. Covariance is frequently measured by the correlation coefficient given by

$$\text{cov}[S_N(\omega_1), S_N(\omega_2)] / (\text{var}[S_N(\omega_1)] \cdot \text{var}[S_N(\omega_2)])^{1/2}$$

where

$$\text{cov}[x,y] = E [(x - \bar{x})(y - \bar{y})].$$

Intuitively, at least, covariance is a measure of resolution, i.e., if $S_N(\omega_1)$ and $S_N(\omega_2)$ have non-zero correlation, they are somewhat "contaminated" by one another. It can be shown that asymptotically $S_N(\omega_1)$ and $S_N(\omega_2)$ are uncorrelated if $|\omega_1 - \omega_2| \geq \frac{2\pi}{mT}$ (independent of the lag window used).

(5) Bandwidth

Bandwidth is another measure (as is correlation) of the ability of S_N to "resolve" peaks of S . It is a non-statistical concept which is window dependent. There are various measures of bandwidth used in spectral analysis but they all are based on the fact that spectrograph estimator can, at least approximately, be put in the form

$$S_N(\omega) = \int_{-\pi}^{\pi} W_N(y) I_N(y) dy$$

where W_N is called the spectral window (the Fourier transform of the lag window). If one considers the periodogram I_N as containing the maximum "information" about S , then this representation states that S_N is obtained by "smearing" or averaging the periodogram over a band of frequencies given roughly by a width figure for W_N (and hence the reason for its name "spectral window"). A frequently used width figure, β , (see Parzen (1961)) is given by $1/2$ the base of a rectangle with the same area as W_N and with height $W_N(0)$. For a truncated estimator this is

$$\beta[S_N] = \frac{2\pi}{mT} \int_{-1}^1 h(t) dt$$

where h is as defined above. Usually $\int_{-1}^1 h(t)dt$ is approximately 1, thus it can be seen that bandwidth is approximately equal to the correlation "distance", i.e., the distance between uncorrelated estimates $S_N(\omega_1), S_N(\omega_2)$.

It is important to note that resolution or correlation is related to the performance of $S_N(\omega)$ at $\omega = 0$. Strictly speaking, $S_N(\omega)$ is statistically only twice as "bad" at 0 and $\frac{2\pi}{mT}$ than elsewhere. (This factor of 2 is due essentially to the fact that, since S is even, it can be considered as folded at $\omega = 0$ and the estimate of $S(-\omega)$ is "folded into" the estimate of $S(\omega)$.) On the other hand, one can say that the estimate $S_N(\epsilon)$ where $0 < \epsilon < \frac{2\pi}{mT}$ is no good because of bandwidth considerations. One can also interpret bandwidth as meaning that since one cannot "resolve" frequencies which are closer together than $\frac{2\pi}{mT}$, one cannot, in fact resolve any frequency less than $\frac{2\pi}{mT}$, i.e., $\frac{2\pi}{mT}$ is the lowest frequency for which one can obtain a reliable estimate. As a matter of fact, this is an optimistic estimate, since usually the time series under investigation is not strictly "stationary". For example, the time series typically has a "slowly varying mean value" (whatever this means) which must be removed prior to spectral analysis. The removal process is usually not completely successful, i.e., there remains a residual non-zero mean which causes the estimates near $\omega=0$ to be strongly biased. Thus to be on the safe side, the limiting low frequency should be several times $\frac{2\pi}{mT}$.

References

- Ables, J.G. (1974) "Maximum entropy spectral analysis", Astron. Astrophys. Suppl. Series 15, 383-393. Also Childers (1978), 23-33
- AFGL - Compilation of papers presented by the Space Physics Division at the Ionospheric Effects Symposium (IES 1978) AFGL-Tr-78-0080, Space Physics Division, Air Force Geophysics Laboratory, Hanscom AFB, Mass.
- Barrett, T.B. (1973) "Multiple convolution using the discrete Fourier transform", Technical Memorandum No. 6, Parke Mathematical Laboratories, Inc., Box A, Carlisle, Mass.
- Barrett, T.B. (1978) "SIGPRODS Reference Manual", Technical Memorandum No. 30, Parke Mathematical Laboratories, Inc., Box A, Carlisle, Mass.
- Bartlett, M.S. (1950) "Periodogram analysis and continuous spectra", Biometrika 37, 1-16
- Beran, M.J. (1968) "Statistical Continuum Theories": Inter-science Publishers, New York
- Blackman, R.B., Tukey, J.W. (1959) "The Measurement of Power Spectra from the Point of View of Communications Engineering", Dover, New York
- Born, M., Wolf, E. (1964) "Principles of Optics": MacMillan, New York
- Childers, D.G. (1978) "Modern Spectrum Analysis", IEEE Press, The Institute of Electrical and Electronics Engineers, Inc., New York (also distributed by Wiley, New York)
- deWolf, D.A. (1975) "Propagation regimes for turbulent atmospheres", Radio Science 10, 53-57
- Frisch, U. (1968) "Probabilistic Methods in Applied Mathematics", Vol. 1, Bharucha-Reid, A.T. (ed.): Academic Press, New York
- Grenander, U., Rosenblatt, M. (1957) "Statistical Analysis of Stationary Time Series", John Wiley, New York
- Ishimaru, A. (1978) "Wave Propagation and Scattering in Random Media", Vol. 1 (Single Scattering and Transport Theory), Vol. 2 (Multiple Scattering, Turbulence, Rough Surfaces, and Remote Sensing): Academic Press, New York
- Jackson, J.D. (1962) "Classical Electrodynamics": John Wiley & Sons, New York
- Jenkins, G.M., Watts, D.G. (1968) "Spectral Analysis and Its Applications", Holden-Day, San Francisco

- Koopmans, L.H. (1974) "The Spectral Analysis of Time Series", Academic Press, New York
- Mercier, R.P. (1962) "Diffraction by a screen causing large random phase fluctuations", Proc. Cambridge Phil. Soc. 58, 382-400
- Modesitt, G. (1971) "Moliere approximation for wave propagation in turbulent media", J. Opt. Soc. Am. 61, 797
- Papoulis, A. (1962) "The Fourier Integral and Its Applications", McGraw-Hill, New York
- Parzen, E. (1961) "Mathematical considerations in the estimation of spectra", Technometrics 3, 167-190. (Also in Parzen, E. (1967), "Time Series Analysis Papers": Holden Day,
- Proceedings of the RADC Spectrum Estimation-Workshop 24,25 & 26 May 1978 (no editor) (Can be obtained from DDC under AD number ADA054650)
- Salpeter, E.E. (1967) "Interplanetary Scintillations", Astrophys.J. 147, 433-448
- Singleton, R.C. (1969a) "An ALGOL convolution procedure for the fast Fourier transform (Algorithm 345)", Comm. ACM 12, 179-184
- Singleton, R.C. (1969b) "Remarks on algorithm 345, an ALGOL convolution procedure based on the fast Fourier transform, Comm. ACM 12, 566
- Tatarski, V.I. (1961) "Wave Propagation in a Turbulent Medium" (Translated by R.A. Silverman): Dover Publications, New York
- Taylor, G.I. (1938) "The spectrum of turbulences", Proc. Roy. Soc. London A132, 476-490
- Taylor, L.S. (1975) "Effects of layered turbulence on oblique waves", Radio Science 10, 121-128
- Thomson, D.J. (1977) "Spectrum estimation techniques for characterization and development of WT4 waveguide I and waveguide II", Bell System Tech. J. 56, 1769-1815 and 1983-2005
- Woodroffe, M.G. and VonNess, J.W. (1967) "The maximum deviation of sample spectral densities", Ann. Math. Stat. 38, 1558-1569
- Wyngaard, J.C., Clifford, S.F. (1977) "Taylor's hypothesis and high frequency turbulence spectra", J. Atmos. Sci. 34, 922
- Yeh, K.C., Liu, C.H. (1972) "Theory of Ionospheric Waves": Academic Press, New York

APPENDIX A

Calculation of the Parameters γ , L , v , α

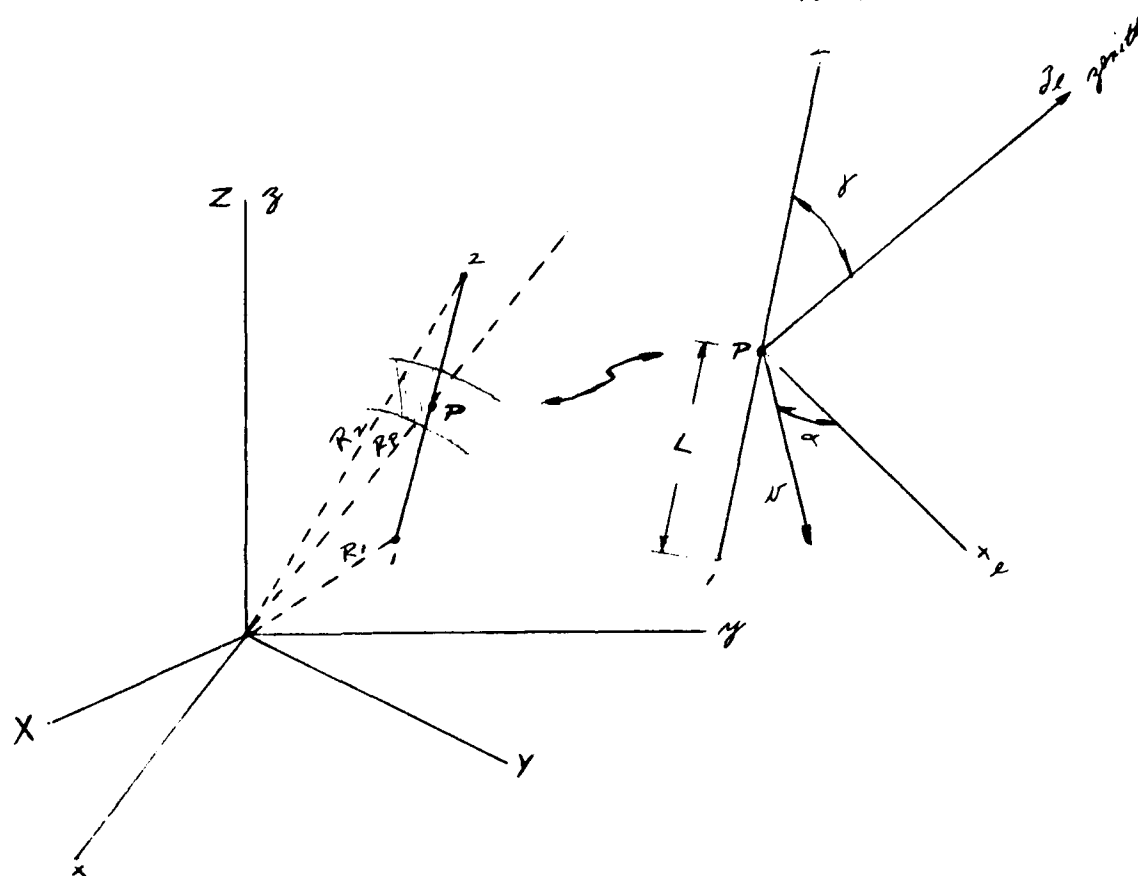


Figure 1

The position and motion of the satellite at point 2 are defined by its coordinates X, Y, Z in a (celestial) inertial coordinate system, and its velocity components $\dot{X}, \dot{Y}, \dot{Z}$ in this system.

The position and motion of the aircraft at point 1 are defined by aircraft height (h_a), geographic latitude (ϕ_a), geographic longitude (λ_a), ground speed (v_a) and direction with respect to geographic north (α_a). (The direction is assumed to be the direction of the ground path - not necessarily the actual aircraft heading.

The scintillation layer is "defined" by its height above the earth h_s and its motion by v_s , α_s where v_s is its speed of motion and α_s its direction of motion with respect to geographic north.

The point P is the point where the transmission path (line \overline{ZI}) intersects the scintillation layer. The motion of the point P relative to the scintillation layer must be found as well as the distance, L, between P and I, and the angle, γ , between the zenith at P and the transmission path. The motion of P is to be obtained as speed, v, and direction, α , relative to the local x-axis defined to lie in the plane defined by $\overline{P, Z}$ and $\overline{P, \text{zenith}}$.

It is assumed that during an observation period, the quantities γ , L, v and α remain constant.

In the following derivations, an earth centered coordinate system, fixed to the earth, is used (this is called the computation system). The relationship between this system (x,y,z) and the celestial system (X,Y,Z) is given by the Greenwich Sidereal Time (here defined as an angle, θ_G) and the earth's rotational speed

$$\Omega_e = \frac{d\theta_G}{dt}.$$

For determining the aircraft position in the computation system, the earth is considered to be the standard ellipsoid. All units are assumed to be compatible, e.g., distances in kilometers, angles in radians and time in seconds.

(a) Conversion of satellite position and motion to the computation system.

$$\begin{aligned}x_2 &= X \cos \theta_G + Y \sin \theta_G \\y_2 &= -X \sin \theta_G + Y \cos \theta_G \\z_2 &= Z \\\dot{x}_2 &= \dot{X} \cos \theta_G + \dot{Y} \sin \theta_G + y_2 \Omega_e \\\dot{y}_2 &= -\dot{X} \sin \theta_G + \dot{Y} \cos \theta_G - x_2 \Omega_e \\\dot{z}_2 &= \dot{Z}\end{aligned}$$

(b) Conversion of aircraft position and motion to the computation system.

$$\begin{aligned}x_1 &= (u+h_a) \cos \phi_a \cos \lambda_a \\y_1 &= (u+h_a) \cos \phi_a \sin \lambda_a \\z_1 &= [u(1-e^2)+h_a] \sin \phi_a\end{aligned}$$

where

$$u = \frac{a_m}{(1-e^2 \sin^2 \phi_a)^{1/2}}$$

$$a_m = \text{semi major axis} = 6378.16 \text{ km}$$

$$e = 2f - f^2 = \text{eccentricity where } f = \frac{1}{298.25}$$

$$\begin{aligned}\dot{x}_1 &= -(u+h_a) [\cos \phi_a \sin \lambda_a \dot{\lambda}_a + \sin \phi_a \dot{\phi}_a \cos \lambda_a] \\\dot{y}_1 &= (u+h_a) [\cos \phi_a \cos \lambda_a \dot{\lambda}_a - \sin \phi_a \dot{\phi}_a \sin \lambda_a] \\\dot{z}_1 &= [u(1-e^2)+h_a] \cos \phi_a \dot{\phi}_a\end{aligned}$$

where

$$\dot{\phi}_a \approx \frac{v_a}{R_a} \cos \alpha_a$$

$$\dot{\lambda}_a \approx \frac{v_a}{R_a} \frac{\sin \alpha_a}{\cos \phi_a}$$

$$R_a = u + h_a$$

(c) Computation of the point P coordinates and motion.

$$(1) \quad \vec{P} = \vec{P}_1 + \alpha (\vec{P}_2 - \vec{P}_1)$$

$$(2) \quad \vec{P} \cdot \vec{P} = R_P^2 \approx (a_m + h_S)^2$$

where \vec{P} , \vec{P}_1 , \vec{P}_2 are the vectors to points P, 1, 2 from the origin. The quantity $0 < \alpha < 1$ is to be computed.

Substituting (1) into (2), the following expression for α results:

$$a\alpha^2 + b\alpha + c =$$

$$(R_2^2 + R_1^2 - 2\vec{P}_1 \cdot \vec{P}_2)\alpha^2 + 2(\vec{P}_1 \cdot \vec{P}_2 - R_1^2)\alpha + R_1^2 - R_P^2 = 0$$

Solve for α , subject to $\alpha < 1$ and then for $\dot{\alpha}$ using the following expression:

$$\dot{\alpha} = \left(\frac{b}{2} + \frac{b\dot{b} - 2\dot{a}c}{2a\alpha + b} - \alpha \dot{a} \right) / a$$

where

$$\dot{a} = 2\vec{P}_2 \cdot \dot{\vec{P}}_2 - 2\vec{P}_1 \cdot \dot{\vec{P}}_2 - 2\vec{P}_1 \cdot \dot{\vec{P}}_2$$

$$b = 2(\vec{P}_1 \cdot \dot{\vec{P}}_2 + \dot{\vec{P}}_1 \cdot \vec{P}_2)$$

Note that in deriving the above expressions, it is assumed that R_1 is constant but R_2 , in general, is not.

From (1) obtain

$$x_P = x_1 + \alpha(x_2 - x_1)$$

$$y_P = y_1 + \alpha(y_2 - y_1)$$

$$z_P = z_1 + \alpha(z_2 - z_1)$$

$$\dot{x}_P = \dot{x}_1 + (x_2 - x_1)\dot{\alpha} + \alpha(\dot{x}_2 - \dot{x}_1)$$

$$\dot{y}_P = \dot{y}_1 + (y_2 - y_1)\dot{\alpha} + \alpha(\dot{y}_2 - \dot{y}_1)$$

$$\dot{z}_P = \dot{z}_1 + (z_2 - z_1)\dot{\alpha} + \alpha(\dot{z}_2 - \dot{z}_1)$$

Next determine the latitude and longitude of the point P and rate of change of these quantities.

$$\phi_P = \frac{\pi}{2} - \cos^{-1}(z_P/R_P)$$

$$\lambda_P = \tan^{-1}(y_P/x_P)$$

$$\dot{\phi}_p = \dot{z}_p / \sqrt{x_p^2 + y_p^2}$$

$$\dot{\lambda}_p = \frac{x_p \dot{y}_p - y_p \dot{x}_p}{x_p^2 + y_p^2}$$

From this, determine the speed and direction of the point P relative to a stationary layer. (Direction is relative to the computation system, i.e., the local meridian through P.)

$$\alpha_p = \tan^{-1} \left(\frac{\dot{\lambda}_p}{\dot{\phi}_p} \cos \phi_p \right)$$

$$v_p = R_p \dot{\lambda}_p \frac{\cos \phi_p}{\sin \alpha_p}$$

Next determine the velocity \vec{v}_1 (speed and direction) of the point, P, relative to the moving scintillation layer. This is given by the vector $\vec{v}_p - \vec{v}_s$ where $\vec{v}_p \equiv (v_p, \alpha_p)$, $\vec{v}_s \equiv (v_s, \alpha_s)$.

$$\vec{v}_1 = (v_1, \alpha_1) \text{ where}$$

$$v_1 = [v_p^2 + v_s^2 - 2v_p v_s \cos(\alpha_p - \alpha_s)]^{1/2}$$

$$\alpha_1 = \tan^{-1} \left(\frac{v_p \cos \alpha_p - v_s \cos \alpha_s}{v_p \sin \alpha_p - v_s \sin \alpha_s} \right)$$

Finally, determine the velocity of P in the local coordinate system (see Figure 2).

$$\theta_2 = \cos^{-1}(z_2/R_2)$$

$$\lambda_2 = \tan^{-1}(y_2/x_2)$$

$$\alpha_x = Q + \pi$$

$$\cos(t) = \cos\theta_p \cos\theta_2 + \sin\theta_p \sin\theta_2 \cos(\lambda_2 - \lambda_p)$$

$$Q = \cos^{-1} \left(\frac{\cos\theta_2 - \cos\theta_p \cos(t)}{\sin\theta_p \sin t} \right)$$

where $\theta_p = \frac{\pi}{2} - \phi_p$ is the colatitude of P.

Finally,

$$\alpha = \alpha_x - \alpha_1$$

The quantities L and γ are found from

$$L = ((x_p - x_1)^2 + (y_p - y_1)^2 + (z_p - z_1)^2)^{1/2}$$

$$\gamma = \cos^{-1} \frac{(x_p - x_1)x_p + (y_p - y_1)y_p + (z_p - z_1)z_p}{LR_p}$$

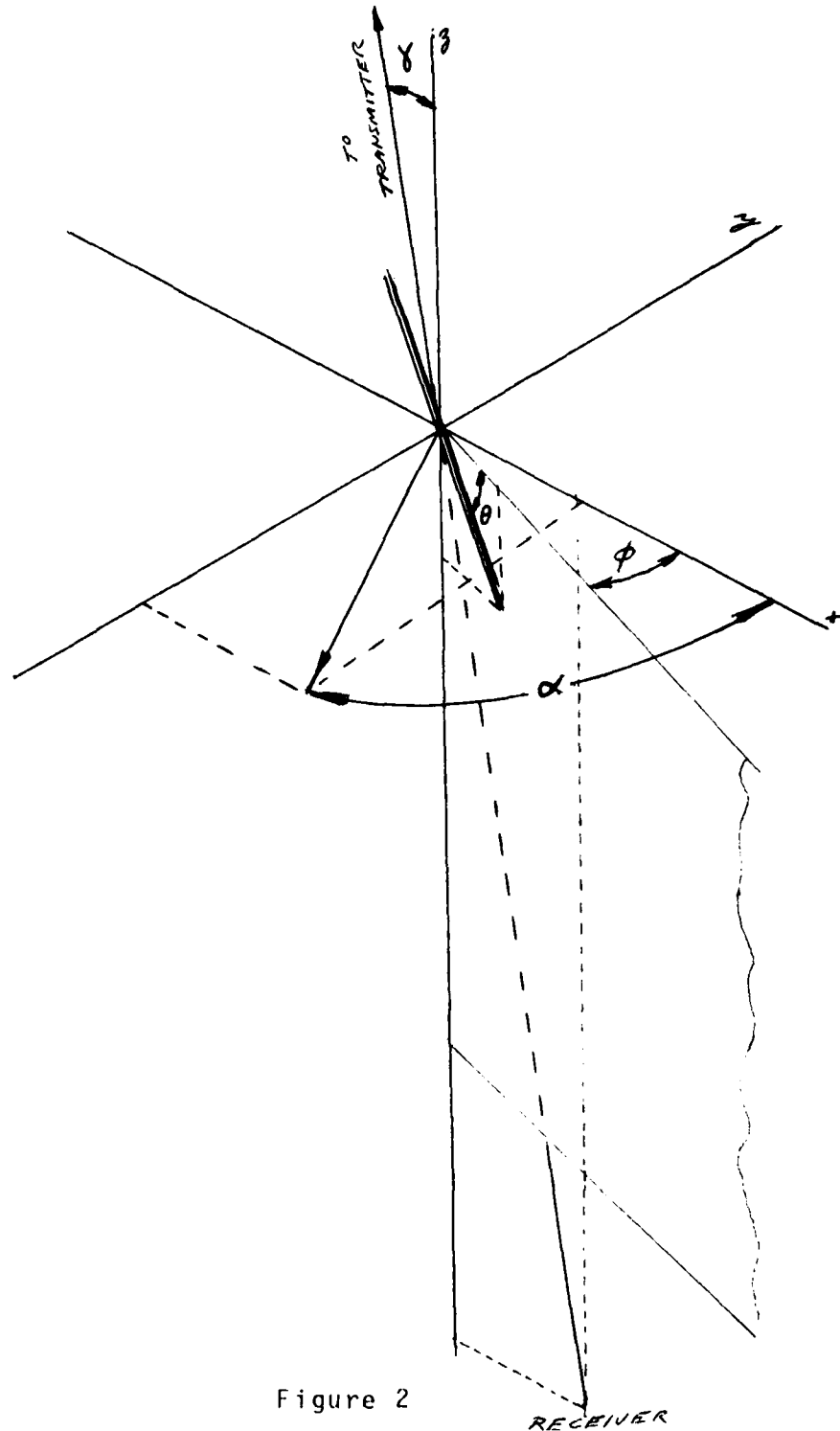


Figure 2

Local coordinate system with origin at the top of the random "screen". The "correlation blob" has semi-major axis, a , in the θ, ϕ direction as shown.

APPENDIX B -- Computation of Theoretical Spectra

A procedure to compute the theoretical spectral density function, $S(\omega)$ (actually $S(f) = S(\frac{\omega}{2\pi})$) as given in Section V is shown below. The bulk of the computations is done by device DISS, PML355 which in turn uses IMSL subroutine DCADRE, to perform the required integration. The parameters used in this procedure are partitioned into two classes -- geometrical and layer. The geometrical parameters are those which define the locations and motions of the transmitter (satellite) and receiver (aircraft). (The transmitter frequency is also included among the geometrical parameters.) Using the geometrical parameters, the necessary "secondary" parameters can be computed using the algorithm in Appendix A. The second set of parameters, the layer parameters, describe the turbulent medium in terms of various correlation function coefficients as well as layer height, thickness and motion. Refer to figures 3a,b,c of Section V and figure 2 of Appendix A for the meaning of parameters THETA, PHI, A, P1 and P2. Note that the procedure is structured so that the user can produce several spectra at one run by varying up to 3 parameters. This "family" of spectra can then conveniently be displayed on one coordinate frame using the procedure in the PLOT mode. The plots are produced in the same manner as is done for the experimental spectra (in particular, see TM30 (Barrett (1978)) for an example) so that theoretical and experimental spectra can be easily compared.

APPENDIX B - (Attachment 1)

A Procedure to Compute Theoretical Spectra

```
.PROC,SCINTTH,YEAR=76,MONTH=10,DAY=20,HOUR=1,MINUTE=8,SECOND=0,
HA=30,LAMBDA=$-77$,PHIA=$-11$,VA=470,ALPHAA=45,F=249,MODEL=2,HS=300,
VS=70,ALPHAS=90,THETA=0,PHI=0,A=10,D=10,P1=3,P2=0,
NN1=5,NN2=1,NN3=1,NP1=11,NP2=1,NP3=1,
P12=150,P13=$-81$,P14=90,P15=$-135$,
P22=0,P23=0,P24=0,P25=0,P32=0,P33=0,P34=0,P35=0,
PLOT=$-1$/$1$,LIB=$JL/IN/SI/IM$,ID=,INPUTF=#DATA,
DEBUG=F/T,SUP=0/1,SWITCH1=OFF/ON,REDINK=OFF/ON.
```

```
*
* REVISION -- JANUARY 29,1980
* AUTHOR -- BARRETT,TB
* PURPOSE -- RUN (AND DISPLAY) THE SPECTRAL DENSITY FOR VARIOUS
* THEORETICAL LAYER MODELS AND EXPERIMENTAL GEOMETRIES.
```

```
*
* PARAMETERS --
* (DEFAULTS SHOWN IN PARENS, THOSE WITH . CAN BE GIVEN AS FLOAT)
```

```
* (1) YEAR (76) YEAR OF EXPERIMENT
* (2) MONTH (10) MONTH OF "
* (3) DAY (20) DAY OF "
* (4) HOUR (1) HOUR OF "
* (5) MINUTE (8) MINUTE OF "
* (6) SECOND (0.) SECOND OF "
```

```
* THE ABOVE PARAMETERS ARE USED TO OBTAIN SATELLITE DATA
```

```
* (7) HA (30.) AIRCRAFT HEIGHT (THOUSANDS OF FEET)
* (8) LAMBDA (-77.) AIRCRAFT LATITUDE (DEGS), - IS SOUTH OF EQ.
* (9) PHIA (-11.) AIRCRAFT LONGITUDE (DEGS), - IS WEST OF GR.
* (10) VA (470.) AIRCRAFT GROUND SPEED (KNOTS)
* (11) ALPHAA (45.) AIRCRAFT HEADING (DEGS CLOCKWISE OF NORTH)
* (12) F (249.) TRANSMITTER FREQUENCY (MHZ)
```

```
* LAYER PARAMETERS --
```

```
* (13) MODEL (2) 1=>GAUSSIAN,2=>POWER LAW,3=>KOLMOGOROF
* (14) HS (300.) LAYER HEIGHT (KM)
* (15) VS (70.) LAYER SPEED (METERS/SEC)
* (16) ALPHAS (90.) LAYER DIRECTION OF MOTION (DEG WRT GEO. N.)
* (17) THETA (0.) VERTICAL TILT OF "CORRELATION BLOB" (DEGS)
* (18) PHI (0.) "SLEW ANGLE" (DEGS) OF THE "CORRELATION BLOB"
* FROM THE "LOCAL" X-AXIS.
* (19) A (10.) CORRELATION BLOB AXIS RATIO (>1)
* (20) D (10.) LAYER THICKNESS (KM)
* (21) P1 (4.) CHARACTERISTIC CORRELATION LENGTH OR OUTER
* SCALE LENGTH (KM)
* (22) P2 (1.) INNER SCALE LENGTH (METERS)
```

```
* THE FOLLOWING PARAMETERS PERMIT VARIATIONS IN UP TO 3 PARAMETERS.
```

```
* NN1 (5) TOTAL NUMBER OF 1ST PARAMETER (1 TO 5)
* NN2 (1) TOTAL NUMBER OF 2ND PARAMETER (1 TO 5)
* NN3 (1) TOTAL NUMBER OF 3RD PARAMETER (1 TO 5)
```

```

.*      NP1      (11)      PARAMETER TO BE VARIED
.*      NP2      (1)      ETC. FOR 2ND AND 3RD PARAMETERS.
.*      NP3      (1)
.*      P12      (150.)   VALUE OF FIRST VARIATION OF FIRST PARAM.
.*      P13      (-81.)   SECOND
.*      P14      (90.)    THIRD
.*      P15      (-135.)  FOURTH
.*      P22 - P25
.*      P32 - P35          SIMILARLY FOR THE OTHER VARIED PARAMETERS.
.*                          THESE ARE ALL DEFAULTED TO 0.
.*      LIB      ($JL/IN/SI/IM$) LIBRARY LOCAL FILE NAMES TO BE USED.
.*      PLOT      (-1/$1.$) IF PLOT IS SPECIFIED PLOTS ARE PRODUCED.
.*      ID        (NULL)   IF SPECIFIED, TAPE3 FROM DISS IS CATALOGED
.*                          UNDER THIS ID (AS TAPE3,ID=ID)
.*      DEBUG     (F/T)    IF SPECIFIED, DEBUG INFO IS PRODUCED.
.*      SUP       (0/1)    IF SPECIFIED, IMSL ERRORS GOTO TAPE1
.*      SWITCH1   (OFF/ON) IF SPECIFIED, PLOTS ARE SINGLE COLOR.
.*      REDINK    (OFF/ON) IF SPECIFIED, PLOTS ARE IN RED INK
.*                          (SWITCH1 SHOULD ALSO BE ON)
.*
.* *****
.* *****E X A M P L E *****
.*
.* BARTH,CM120000,T511.
.* ATTACH(JL,JURGLIBX3693818,ID=BANDES)
.* ATTACH(IN,INFOLIBX3693818,ID=BANDES)
.* ATTACH(SI,SIGLIBX3693818,ID=WONG)
.* ATTACH(IM,IMSLLIBX3693818,ID=WONG)
.* LIBRARY(JL)
.* ATTACH(SATFIL,Y76M10D20X3693818,ID=BANDES)
.* SCINTTH,ID=BARRETT,PLOT.
.*
.* *****
.*
.* IFE,$SWITCH1$=$ON$,LAB0.
.* SWITCH(1)
.* ENDIF,LAB0.
.* REQUEST(TAPE3,*PF)
.* FTN(I=INPUTF,SYSEDIT,R=3,SL,L=Q)
.* LDSET(#LIB=LIB)
.* LGO(PL=60000)
.* EXIT(U)
.* IFE,$DEBUG$=$T$,LAB3.
.* REVERT.
.* ENDIF,LAB3.
.* RETURN(LGO)
.* IFE,$ID$.NE.$$ ,LAB1.
.* CATALOG(TAPE3,#ID=ID)

```

```

ENDIF, LAB1.
IFE, $PLOTS$.EQ.$1.$, LAB2.
ATTACH (PEN, ONLINEPEN)
ATTACH (PLT, PLOTLIB)
LIBRARY (PEN, PLT)
REQUEST (#PLOT, *Q)
IFE, $REDINKS=$OFF$, LAB4.
DISPOSE (#PLOT, *OL)
ELSE, LAB4.
DISPOSE (#PLOT, *PL)
ENDIF, LAB4.
ENDIF, LAB2.
FTN (I=INPUTF, SYSEDIT, R=3, SL, L=Q)
LDSET (PRESET=0, #LIB=LIB, SUBST=GENGENU-GENGEN4)
LGO (PL=60000)
REWIND (TAPE2)
COPY (TAPE2)
REWIND (Q)
COPY (Q)
EXIT.
DMP (60000)
REWIND (TAPE2)
COPY (TAPE2)
REWIND (Q)
COPY (Q)
.DATA
PROGRAM RUNDIS (OUTPUT=64, TAPE3, SATFIL, TAPE1=64)
COMMON/GEOLAY/GL (22, 5)
COMMON/PHIAUX1/#DEBUG
LOGICAL #DEBUG
DIMENSION IGL (22, 5)
EQUIVALENCE (GL, IGL)
#DEBUG=.DEBUG.
NY=NN1*NN2*NN3
DO 90 I=1, NY
IGL (1, I)=YEAR
IGL (2, I)=MONTH
IGL (3, I)=DAY
IGL (4, I)=HOUR
IGL (5, I)=MINUTE
GL (6, I)=SECOND
GL (7, I)=HA
GL (8, I)=LAMRDA
GL (9, I)=PHIA
GL (10, I)=VA
GL (11, I)=ALPHAA
GL (12, I)=F
IGL (13, I)=MODEL
GL (14, I)=HS

```

```

GL(15,I)=VS
GL(16,I)=ALPHAS
GL(17,I)=THETA
GL(18,I)=PHI
GL(19,I)=A
GL(20,I)=D
GL(21,I)=P1
GL(22,I)=P2
90  CONTINUE
    IF (NN1 .EQ. 1) GOTO 600
    IF ((NP1 .LT. 6) .O. (NP1 .EQ. 13)) GOTO 100
    GL(NP1,2)=P12
    GL(NP1,3)=P13
    GL(NP1,4)=P14
    GL(NP1,5)=P15
    GOTO 200
100  IGL(NP1,2)=P12
    IGL(NP1,3)=P13
    IGL(NP1,4)=P14
    IGL(NP1,5)=P15
200  IF (NN2 .EQ. 1) GOTO 600
    IF ((NP2 .LT. 6) .O. (NP2 .EQ. 13)) GOTO 300
    GL(NP2,2)=P22
    GL(NP2,3)=P23
    GL(NP2,4)=P24
    GL(NP2,5)=P25
    GOTO 400
300  IGL(NP2,2)=P22
    IGL(NP2,3)=P23
    IGL(NP2,4)=P24
    IGL(NP2,5)=P25
400  IF (NN3 .EQ. 1) GOTO 600
    IF ((NP3 .LT. 6) .O. (NP3 .EQ. 13)) GOTO 500
    GL(NP3,2)=P32
    GL(NP3,3)=P33
    GL(NP3,4)=P34
    GL(NP3,5)=P35
    GOTO 600
500  IGL(NP3,2)=P32
    IGL(NP3,3)=P33
    IGL(NP3,4)=P34
    IGL(NP3,5)=P35
600  CALL DISS(NN1,NN2,NN3,NP1,NP2,NP3,SUP)
    END
.EOR
PROGRAM TESTGEN(OUTPUT=64,TAPE2=64,TAPE3)
COMMON DATA(7000)
COMMON/CONTROL/IC(100)
COMMON/AUXIL/IA(10)

```

```

COMMON/PROCON/IPR(700)
COMMON/PRINT/IPRNT(300)
COMMON/FIT/FIT(600)
COMMON/SUB/SUB,M1,L1,IWHER(5)
COMMON/MINPLT/MINPLT(10)
COMMON/GENGENA/IWHERE
DIMENSION PRNT(300)
EQUIVALENCE (IPRNT,PRNT)
DATA (IPR=256,100.,9.,2,6,50)
DATA (IPRNT=PLOT,0,1,"LOG",-1.,4.,0.,1,0,1,"LOG",-8.,1.,1.)
IWHERE=3000
NY=NN1*NN2*NN3
IPRNT(2)=IPRNT(9)=NY
IF (NY .EQ. 1) GOTO 100
K=15
DO 110 I=2,NY
  IPRNT(K)=I
  PRNT(K+1)=PRNT(11)
  PRNT(K+2)=PRNT(12)
  PRNT(K+3)=PRNT(13)
  PRNT(K+4)=PRNT(14)
  K=K+5
110 CONTINUE
100 CALL GENGEN(1,1,1,270,1,0,NVAL)
  IF (IPR(7) .EQ. 0) GOTO 100
  CALL FINISH
END

```

APPENDIX C -- Computation of the Spectral Density Function Estimates

The estimator which was used is that given by equation 7.7 in Section VII. For technical reasons we write this equation in the form:

$$(1) \quad S_N(\omega) = \frac{1}{2\pi} \sum_{n=-2m_N+1}^{2m_N-1} w(n/m_N) R_N(n) e^{-in\omega}$$

(Note that $2m_N$ is the actual truncation point rather than m_N because w has been "normalized" to be 0 for $|x| \geq 2$ rather than for $|x| \geq 1$ as in Equation (7.7). More will be said about w later.) Let $C_N(n) = w(n/m_N) \cdot R_N(n)$ and consider S_N evaluated at the points

$$\pi j / m_N \quad j=0, \dots, 2m_N-1.$$

Then:

$$(2) \quad \begin{aligned} S_N\left(\frac{\pi j}{m_N}\right) &= \frac{1}{2} \sum_{n=-2m_N+1}^{2m_N-1} C_N(n) e^{-i\pi n j / m_N} \\ &= \frac{1}{\pi} \sum_{n=0}^{2m_N-1} C_N(n) \cos\left(\frac{\pi n j}{m_N}\right) - \frac{C_N(0)}{2\pi} \end{aligned}$$

Since $m_T = 2m_N$, we can write

$$\begin{aligned} S_N\left(\frac{2\pi j}{m_T}\right) &= \frac{1}{\pi} \sum_{n=0}^{m_T-1} C_N(n) \cos\left(\frac{2\pi n j}{m_T}\right) - \frac{C_N(0)}{2\pi} \\ &= \frac{1}{\pi} \operatorname{Re} \{ \text{DFT}_{m_T} C_N \} (j) - \frac{C_N(0)}{2\pi} \end{aligned}$$

$$j=0, \dots, m_T-1.$$

Note that since C_N is real, $\text{Re}\{\text{DFT}_{m_T} C_N\}$ is even (see Appendix A of Barrett (1973)) and hence S_N needs to be evaluated only at the points $j=0, \dots, m_T/2 = m_N$. Of course, using the FFT algorithm S_N is found at all points $j=0, \dots, m_T-1$ and $\text{Im}\{\text{DFT}_{m_T} C_N\}$ is computed whether one wants it or not. We are concerned mainly with evaluating S_N at the points $\pi j/m_N$ because of correlation considerations mentioned in Section VII. It is interesting to note, however, that knowledge of $\text{Re}\{\text{DFT}_{m_T} C_N\}$ and $\text{Im}\{\text{DFT}_{m_T} C_N\}$ is necessary and sufficient for evaluating S_N over the continuum $[0, \pi]$ because of the "sampling theorem" (see Appendix A of Barrett (1973)).

In this next section we will be concerned mainly with the computation of the correlograms R_N . First, remember that the theoretical properties of this class of estimators are based on their asymptotic behavior as N , the length of the time series (or "amount of data") N becomes larger and larger. Second, note that the truncation point m_T must grow larger at a much smaller rate than N for good asymptotic behavior of S_N . This means that it is not necessary to compute the correlogram $R_N(n)$ for all possible values of n , and, in fact, as N becomes large, R_N need be calculated over only a relatively small percent of its support. As will be shown, it is convenient to calculate R_N over a fixed interval (say $0, \dots, N_1-1$), where N_1 is equal to or greater than the largest value of the truncation point, regardless of the amount of data available. (It goes without saying that in any finite experiment, the amount of data and hence the truncation point will presumably be the truncation point used in the last "trial" (see below).) The reason for this is that, 1) the FFT is a very efficient algorithm for computing correlations if N_1 is "highly composite" (in the algorithm used this means $N_1=2^k$, k a positive integer), and 2) it is not necessary to recompute "all of" R_N as more data is added. In fact, consider a time series of length N such that $N=\ell N_1$ where ℓ is a positive integer. Then it is apparent (see Figure C1.) that $R_N(n')$ can be written as:

$$R_N(n') = \frac{1}{N} \left[\sum_{k=1}^{\ell} r r_k(n') + \sum_{k=1}^{\ell-1} c r_k(n') \right] = R(n'),$$

$n'=0, \dots, N_1-1$

	0	1	2	3	4	5	6	7	8	9	10	11	12	13	14	15	
	
																	* $\rightarrow R_{16}(3)$
	
	<hr/>																
	0	1	2	3	4	5	6	7									
x_k									* $\rightarrow rr_k(3)$
x_k									
	<hr/>																
									0	1	2	3	4	5	6	7	
x_{k+1}									
																	* $\rightarrow rr_{k+1}(3)$
x_{k+1}									
	<hr/>																
									0	1	2	3	4	5	6	7	
x_k		
																	* $\rightarrow cr_k(3)$
x_{k+1}									
	<hr/>																

* means multiply corresponding data then add. Corresponding data are shown as . in the same columns.

$$R_{16}(3) \equiv R_{2(N_1)}(3) = \frac{1}{16} [rr_k(3) + rr_{k+1}(3) + cr_k(3)] \quad .$$

Figure C1. "Decomposition" of the correlogram for $N_1=8$.

where

$$rr_k(n') = \sum_{n=0}^{N_1-n'-1} x_k(n)x_k(n+n')$$

$$cr_k(n') = \sum_{n=0}^{n'-1} x_k(n+N_1-n')x_{k+1}(n) ,$$

x_k is the k^{th} block of data and the data in each block is numbered from 0 to N_1-1 . Moreover, rr_k and cr_k can be found by "circular" correlation and thus by a double discrete Fourier transform as will be described in some detail below. In fact if

$$f(n) = x_k(n) \quad n=0, \dots, N_1-1$$

$$= 0 \quad n=N_1, \dots, 2N_1-1$$

$$g(n) = x_{k+1}(n) \quad n=0, \dots, N_1-1$$

$$= 0 \quad n=N_1, \dots, 2N_1-1$$

then $rr_k(n') = f \star f(n') \quad n'=0, \dots, N_1-1$

$$cr_k(n') = f \star g(N_1+n') \quad n'=0, \dots, N_1-1$$

where \star means circular correlation for $G=Z_{2N_1}$ (see Appendix A of Barrett (1973)).

In obtaining the spectral density function estimates, two "devices" are used. (A description of these "devices" in the form of comment lines from the source software is given as attachments.) The first one is called CORREL and computes the required correlogram $R_N(n)$ from scintillation data input. The second device, called SPECTR, uses the output of CORREL to

compute the spectral density function estimator, S_N . For technical reasons (storage considerations and run time) it is convenient to make several passes (these were referred to as "trials", ℓ , above) through CORREL, obtaining additional "blocks" of scintillation data each time until R_N has been computed for all required lags. Following this, SPECTR is used to calculate S_N . An example of this process can be found in Barrett (1978), p. 27-33. CORREL, in particular, utilizes many of the symmetry properties of the FFT.

The computations are outlined below. Figure C2 is an array diagram summarizing the major computations and subdivisions. Assume that the $(\ell-1)$ th correlogram has been found and that the discrete Fourier transform $X_{\ell-1}$ of the corresponding block of data is stored. (In the sequel, X_ℓ refers to the discrete Fourier transform of the ℓ th block of data or this transform in reverse binary order. When computing correlograms, it is not necessary to put transforms in correct order; the FFT algorithm used naturally outputs in reverse binary order.) Then two new blocks of data x_ℓ and $x_{\ell+1}$ are produced as described in Barrett (1978) to be used as "input" to CORREL. Zeroes are appended to these data blocks to obtain the equivalent of functions f and g described above. (The same symbol x_ℓ will denote x_ℓ or x_ℓ appended with zeroes; similarly X_ℓ will denote the Fourier transform of x_ℓ appended with zeroes.) The two real "functions" x_ℓ and $x_{\ell+1}$ are simultaneously transformed as described in Appendix A (Barrett (1973)) - (see Fact A). Then $X_\ell \bar{X}_\ell$ and $X_{\ell+1} \bar{X}_{\ell+1}$ are formed and inverse transformed, again simultaneously, to obtain the quantities rr_ℓ and $rr_{\ell+1}$. rr_ℓ is added to $R_{\ell-1} \cdot \ell/(\ell-1)$ and $rr_{\ell+1}$ is stored. Next the quantity $X_{\ell-1} \bar{X}_\ell$ is formed and inverse transformed to obtain $cr_{\ell-1}$ and $R_\ell = R_{\ell-1} \cdot \ell/(\ell-1) + rr_\ell + cr_{\ell-1}$ output. (In performing the inverse transform, Fact B of Appendix A (Barrett (1973)) is used.) Finally $X_\ell \bar{X}_{\ell+1}$ is formed and inverse transformed and $R_{\ell+1}$ found from $R_{\ell+1} = R_\ell \cdot \ell/(\ell+1) + rr_{\ell+1} + cr_\ell$ to complete one cycle through CORREL.

The correlogram computations are based on Comm. A.C.M. algorithm 345, an Algol "convolution" procedure by Singleton (1969a, 1969b). This algorithm consist essentially of four procedures: FFT4 produces the discrete Fourier transform of a complex valued function (in reverse binary order); REVFFT4 produces the inverse DFT of complex data which is in reverse binary order; REALTRAN unscrambles the transform (or inverse transform) if Fact C (Appendix A of Barrett (1973)) is used to find the transform of a real function of even length; REVERSEBINARY (which is not used) is used to return the output of FFT to normal order. Using this nomenclature, CORREL can be summarized as follows:

- 1) x_{ℓ} and $x_{\ell+1}$ are the inputs to FFT4 which outputs X_{ℓ} and $X_{\ell+1}$ in scrambled form. This scrambled output is unscrambled as described in Fact A to obtain X_{ℓ} and $X_{\ell+1}$ which are stored.
- 2) $X_{\ell}\bar{X}_{\ell}$ and $X_{\ell+1}\bar{X}_{\ell+1}$ are used as inputs to REVFFT4 which returns the scrambled versions of rr_{ℓ} and $rr_{\ell+1}$. These are unscrambled as above.
- 3) $X_{\ell-1}\bar{X}_{\ell}$ are formed and then the real function $\text{Re}[X_{\ell-1}\bar{X}_{\ell}] - \text{Im}[X_{\ell-1}X_{\ell}]$. This latter function is made into the real and imaginary parts of a complex function which in turn is inverse transformed by REVFFT4 and "unscrambled" next by REALTRAN to obtain $cr_{\ell-1}$.
- 4) $X_{\ell}\bar{X}_{\ell+1}$ is formed and cr found as above.

Following CORREL, the spectral density function estimate is found by SPECTR. First a subroutine (which may be changed for different lag windows) produces the weighted correlograms, i.e., the $C_N(n)$ referred to in Equation (2). The discrete Fourier transform of C_N is performed using a fast Fourier transform algorithm provided by Norman Brenner formerly of MIT Lincoln Laboratory. This algorithm may be used with data of any length although it works faster with a highly composite length. The original program may be used to transform real or complex valued functions defined on $Z_{N_1} \times Z_{N_2} \times \dots \times Z_{N_m}$ where N_1, N_2, \dots, N_m may

be any integer. SPECTR uses an abridged version of this algorithm which transforms real functions on Z_{N_1} where N_1 is even.

The lag window w which was used, has some nice properties and, in fact, was chosen because of these properties. (See Woodroffe and VanNess (1967).) The Fourier transform of w , the "spectral window" W , is assumed to be non-negative even and continuous with a continuous Fourier transform $\hat{W} = w$ (the "lag window"). In addition, we assume that w has the following properties:

- (a) $w(x) = 0$ $|x| > 2$
- (b) $w(0) = 1$
- (c) $w'(0)$ exists.

The assumptions for W and assumption (b) and (c) for w are conditions imposed by theorem 2.2 of Woodroffe and VanNess (1967). Condition (a) is imposed partly for computational convenience and partly because theorem 2.2 is based on the fact that truncated spectrograph estimators are assumed. Normally, w is truncated at $|x| = 1$; for technical reasons truncation at $|x| = 2$ is used.

A function, w , which satisfies these conditions is that obtained by self-convolving a suitable "triangle" function.

This particular lag window was apparently first proposed by E. Parzen in 1957 (see Parzen (1961)). It is probably the simplest example of a function which meets the conditions.

The Fourier transform of such a function is obviously non-negative since the Fourier transform of the triangle function is non-negative. Let the triangle function be given by:

$$\begin{aligned} \Delta(t) &= a(1 - |t/\tau|) & |t| \leq \tau \\ &= 0 & |t| > \tau. \end{aligned}$$

Then the function obtained from self-convolution of this function is:

$$\begin{aligned}\Delta * \Delta(t) &= a^2 \tau^2 \left(\frac{1}{2} \left(\frac{t}{\tau} \right)^3 - \left(\frac{t}{\tau} \right)^2 + \frac{2}{3} \right) & 0 \leq t \leq \tau \\ &= \frac{a^2 \tau^2}{6} \left(2 - \frac{t}{\tau} \right)^3 & \tau \leq t \leq 2\tau \\ &= 0 & t \geq 2\tau\end{aligned}$$

and by even symmetry for $t < 0$.

If $\tau = 1$ and $a^2 = 3/2$, then we obtain

$$\begin{aligned}w(t) &= \frac{3}{4}t^3 - \frac{3}{2}t^2 + 1 & 0 \leq t \leq 1 \\ &= \frac{1}{4}(2 - t)^3 & 1 \leq t \leq 2 \\ &= 0 & t \geq 2\end{aligned}$$

A	B	C	D	Q3	Q1	
$\frac{x_2}{---}$ 0	$\frac{x_3}{---}$ 0	---	---	$\frac{R_1}{---}$	$\frac{x_1}{---}$ x_1	(1) x_2, x_3 are new data. R_1, x_1 are from previous cycle.
FFT4 plus Fact A						
$\frac{x_2}{---}$ x_2	$\frac{x_3}{---}$ x_3	$\frac{x_2 \bar{x}_2}{---}$	$\frac{x_3 \bar{x}_3}{---}$	$\frac{R_1}{---}$	$\frac{x_1}{---}$ x_1	(2) (Fact A, etc. refer to Appendix A of Barrett (1973).)
REFFT4 plus Fact A						
$\frac{x_2}{---}$ x_2	$\frac{x_3}{---}$ x_3	---	---	$\frac{Q}{---}$ rr_3	$\frac{x_1}{---}$ x_1	(3) $Q = R_1 + rr_2$
Fact B and Fact C						
$\frac{x_2}{---}$ x_2	---	$\frac{x_1 \bar{x}_2}{---}$ (1)	$\frac{x_1 \bar{x}_2}{---}$ (2)	$\frac{Q}{---}$ rr_3	$\frac{x_3}{---}$ x_3	(4) (1) even numbered $x_1 \bar{x}_2$ (2) odd numbered $x_1 \bar{x}_2$
revfft4 and REALTRAN						
$\frac{x_2}{---}$ x_2	---	---	---	$\frac{R_2}{---}$ rr_3	$\frac{x_3}{---}$ x_3	(5) $R_2 = \frac{1}{2}R_1 + rr_2 + cr_1$
If SPECTR called here						
$\frac{x_2}{---}$ x_2	---	---	$\frac{S_2}{---}$	$\frac{R_2}{---}$ rr_3	$\frac{x_3}{---}$ x_3	(6) S_2 output
Fact B and Fact C						
---	---	$\frac{x_2 \bar{x}_3}{---}$ (1)	$\frac{x_2 \bar{x}_3}{---}$ (2)	$\frac{R_2}{---}$ rr_3	$\frac{x_3}{---}$ x_3	(7) (1) even numbered $x_2 \bar{x}_3$ (2) odd numbered $x_2 \bar{x}_3$
REFFT4 and REALTRAN						
---	---	---	---	$\frac{R_3}{---}$	$\frac{x_3}{---}$ x_3	(8) $R_3 = \frac{2}{3}R_2 + rr_3 + cr_2$
If SPECTR called here						
---	---	---	$\frac{S_3}{---}$	$\frac{R_3}{---}$	$\frac{x_3}{---}$ x_3	(9) S_3 output
(Return to (1))						

Figure C2. -- Array use diagram of CORREL and SPECTR.
(Note that each array is shown in two halves since in some stages each half is used to store different data.)

APPENDIX C - (Attachment 1)

Comments from CORREL, the Correlogram Estimator

```
SUBROUTINE CORREL(L,IA,IX,IY,IPRT,IPLT,INDIC,NSIZE,
$  A,B,C,D,Q1,Q3,SINE,IGO)
```

```
C
C PML --      236
C REVISION -- MARCH 6,1979
C AUTHOR --   BARRETT,TB
C PURPOSE --  COMPUTES THE CORRELOGRAM FOR A REAL TIME SERIES
C              WHCIH IS GENERATED IN BLOCKS OF SIZE IBLOCK SUCH THAT
C              IBLOCK IS A POWER OF 2 AND (IBLOCK-1)*IA(1) IS THE
C              MAX. LAG VALUE. THIS DEVICE IS SIGPRODS
C              COMPATIBLE WITH STATE STORED EXTERNALLY, LARGELY
C              IN ARRAY A -> SINE.
C
C USE OF STANDARD ARGUMENTS
C   L   START OF /CONTROL/ TO STORE "STATE" (PARTIALLY)
C       AS FOLLOWS
C       1   INITIAL CALL INDICATOR
C       2   NUMBER OF OUTPUT TERMINALS ON INPUTTING
C           DEVICE
C       3   STARTING LOCATION IN DATA FOR OBTAINING INPUT
C       4   STARTING LOCATION IN DATA FOR STORING OUTPUT
C       5   II=NO. OF BLOCKS WHICH HAVE BEEN PROCESSED
C       6   MZ,(2**MZ)=NZ=2*IBLOCK
C   IA  START OF /AUXIL/ TO OBTAIN AUXILIARY INPUT DATA
C       AS FOLLOWS
C       1   TIME INTERVAL TO BE ASSOCIATED WITH 1 LAG UNIT
C       2   UNITS (HOLLERITH) TO BE ASSOCIATED WITH THE TIME INTERVAL
C           THIS IS STORED AS PART OF THE PIN LABEL FOR
C           LABELING PURPOSES (ONLY USED IF INDIC=2)
C   IX  INPUT TERMINAL LOCATION (NOTE THIS IS A SINGLE
C       INPUT (REAL) DEVICE)
C   IY  OUTPUT TERMINAL (CAN BE AN ARRAY OF LENGTH 2)
C       CONTAINING THE LOCATIONS FOR UP TO 2 OUTPUTS.
C       THE FIRST IS THE MAIN OUTPUT (CORRELOGRAM)
C       WHILE THE SECOND IS THE "TIME BASE" OUTPUT IF
C       INDIC=2
C   IPRT PRINTER NUMBER
C   IPLT RECORDER NUMBER
C USE OF PARTICULAR ARGUMENTS
C   INDIC (1,2,3,4) INDICATING THE MODE OF OPERATION
C       IF INDIC=1 ONLY THE CORRELOGRAM IS PRODUCED.
C       IF INDIC=2 A TIME BASE OUTPUT AND CORRELOGRAM ARE PRODUCED
C       IF INDIC=3 A TIME BASE OUTPUT AND NORMALIZED (TO 1)
C       CORRELOGRAM IS OUTPUT
C       IF INDIC=4 A NORMALIZED CORRELOGRAM AND NO TIME BASE
C       IS PRODUCED.
C   NSIZE IS THE SIZES OF THE ARRAYS A->Q3. NSIZE
```

```

C      SHOULD BE AT LEAST 2*MT+2
C      A->Q3      ARRAYS FOR STORING MOST OF THE STATE OF CORREL
C      SINE      ARRAY FOR STORING VALUES OF FUNCTION SIN
C      (MIN. SIZE M2 FROM 2*MT=2**MZ)
C      IGO SEE OTHER OUTPUT
C      OTHER INPUT ---
C      /PROCON/1      WHICH IS THE DATA BLOCK SIZE IS
C      ASSUMED TO BE THE VALUE OF MT
C      /PROCON/8      IS THE ACTUAL AMOUNT OF DATA GENERATED
C      (NOTE THAT THE LAST BLOCK MAY NOT BE COMPLETELY
C      FILLED WITH DATA)
C      OTHER OUTPUT ---
C      IGO (INDICATOR OUTPUT FOR USE BY OTHER DEVICES AS FOLLOWS)
C      0 => NO CORRELOGRAM, RETURN TO GENERATOR
C      1 => CORRELOGRAM, RETURN TO CORREL
C      2 => CORRELOGRAM, RETURN TO GENERATOR
C      (RETURNS TO GENERATOR ARE CONDITIONAL ON IPR(7)=0)
C      SUBROUTINES (NON-SYSTEM)
C      FFT4      FAST FOURIER TRANSFORM
C      RVFFT4      INVERSE FFT
C      REALTR
C      SPECIAL PRECAUTIONS ---
C      1      /PROCON/1 SHOULD BE A POWER OF 2. IF IT IS NOT
C      THE SUBROUTINE WILL TERMINATE. NOTE HOWEVER
C      THAT THE DATA BLOCK DOES NOT HAVE TO BE COMPLETELY
C      FILLED
C      2      THE ARRAY A->Q3 MUST BE DECLARED IN THE CALLING
C      PROGRAM WITH SUFFICIENT SIZE (SO THAT 2 DATA
C      BLOCKS+2) WILL FIT INTO EACH ARRAY.

```

APPENDIX C - (Attachment 2)

Comments from SPECTR, The SPDF Estimator

```

SUBROUTINE SPECTR(L,IA,IX,IY,IPRT,IPLT,TL,IGO,A,D)
C
C   PML          231
C   REVISION -- JUNE 2, 1977
C   AUTHOR    -- UNKNOWN
C   PURPOSE   -- COMPUTES THE SPECTROGRAM OF A REAL TIME SERIES FROM THE
C                 CORRELOGRAM AS PRODUCED BY CORREL. THIS DEVICE IS SIGPRODS
C                 COMPATIBLE WITH STATE STORED EXTERNALLY. IT HAS TWO OUTPUT
C                 TERMINALS THE FREQUENCY BASE AND THE TIME BASE. NOTE THAT
C                 THIS IS CONSIDERED TO BE ESSENTIALLY A TERMINATING DEVICE
C                 AND IS NOT IN THE "MAIN" SIGNAL FLOW STREAM.
C   USE OF STANDARD ARGUMENTS
C   L   START OF /CONTROL/ TO STORE "STATE"
C       1   INITIAL CALL INDICATOR
C       2   ACTUAL "TIME" INTERVAL
C       3   MT FOR PREVIOUS CALL
C   IA  START OF /AUXIL/ TO OBTAIN AUXILIARY INPUT DATA AS FOLLOWS
C       1   "TIME" INTERVAL ASSOCIATED WITH THE CORRELOGRAM
C           (FLOATING POINT). IF NOT LEGITIMATE IS SET TO 1.
C       2   "TIME" INTERVAL UNITS (HOLLERITH). (NOTE THAT
C           THE UNITS SHOULD BE 8 CHARACTERS OR LESS - LEFT
C           JUSTIFIED
C           THE MAXIMUM FREQUENCY VALUE GENERATED BY SPECTR IS
C           1./(2.*"TIME").
C   IX  INPUT TERMINAL LOCATION IN DATA (INPUT MUST BE
C       CORRELOGRAM OUTPUT
C   IY  OUTPUT TERMINAL (ARRAY OF LENGTH 2)
C       THE FIRST ELEMENT REFERS TO THE LOCATION IN DATA FOR
C       THE SPECTROGRAM WHILE THE SECOND LOCATES THE FREQUENCY
C       BASE OUTPUT.
C   IPRT  PRINTER NUMBER
C   IPLT  RECORDER NUMBER
C   USE OF PARTICULAR ARGUMENTS
C   TL  TRUNCATION TIME, MUST BE LESS THAN IBLOCK*TAU WHERE TAU
C       IS THE SAMPLE INTERVAL (=AI(IA) )
C   IGO =0  DOES NOTHING
C       =1  COMPUTE
C       THIS INDICATOR IS NECESSARY BECAUSE OF THE WAY THAT
C       CORREL INTERACTS WITH THE DATA SOURCE.
C   A,D WORK STORAGE ARRAYS - USUALLY THE SAME ONES USED BY
C       CORREL. (SEE CORREL)
C   OTHER INPUT ---
C   /PROCON/1 WHICH IS THE DATA BLOCK SIZE, IBLOCK, IS
C       ALSO USED TO DETERMINE THE AMOUNT OF DATA OUTPUT (AS
C       WELL AS INPUT). THE NUMBER OF "FUNDAMENTAL" AND UNIQUE
C       FREQUENCIES IS MT/2+1 WHICH AT MOST IS HALF OF IBLOCK.
C       THE OTHER FREQUENCIES ARE FOUND BY INTERPOLATION USING
```

```

C      THE SAMPLING THEOREM.
C  OTHER OUTPUT ---
C      NONE
C  OTHER SUBROUTINES (NON-SYSTEM)
C      FFT GENERAL PURPOSE FFT ALGORITHM FOR REAL DATA
C      ALSO DOES INTERPOLATION)
C      W8AUTO      WEIGHT FUNCTION FOR WEIGHTING THE CORRELOGRAM
C  SPECIAL PRECAUTIONS
C      1  SPECTR CAN ONLY BE ATTACHED TO CORREL OR POSSIBLY A
C          "RECORDER" WHICH HAS STORED THE OUTPUT OF CORREL.
C      2  THE TRUNCATION POINT MUST BE LESS THAN OR EQUAL TO
C          IBLOCK (IPR(1)). IF IT IS NOT THE PROGRAM WILL
C          SET IT TO THIS VALUE.

```